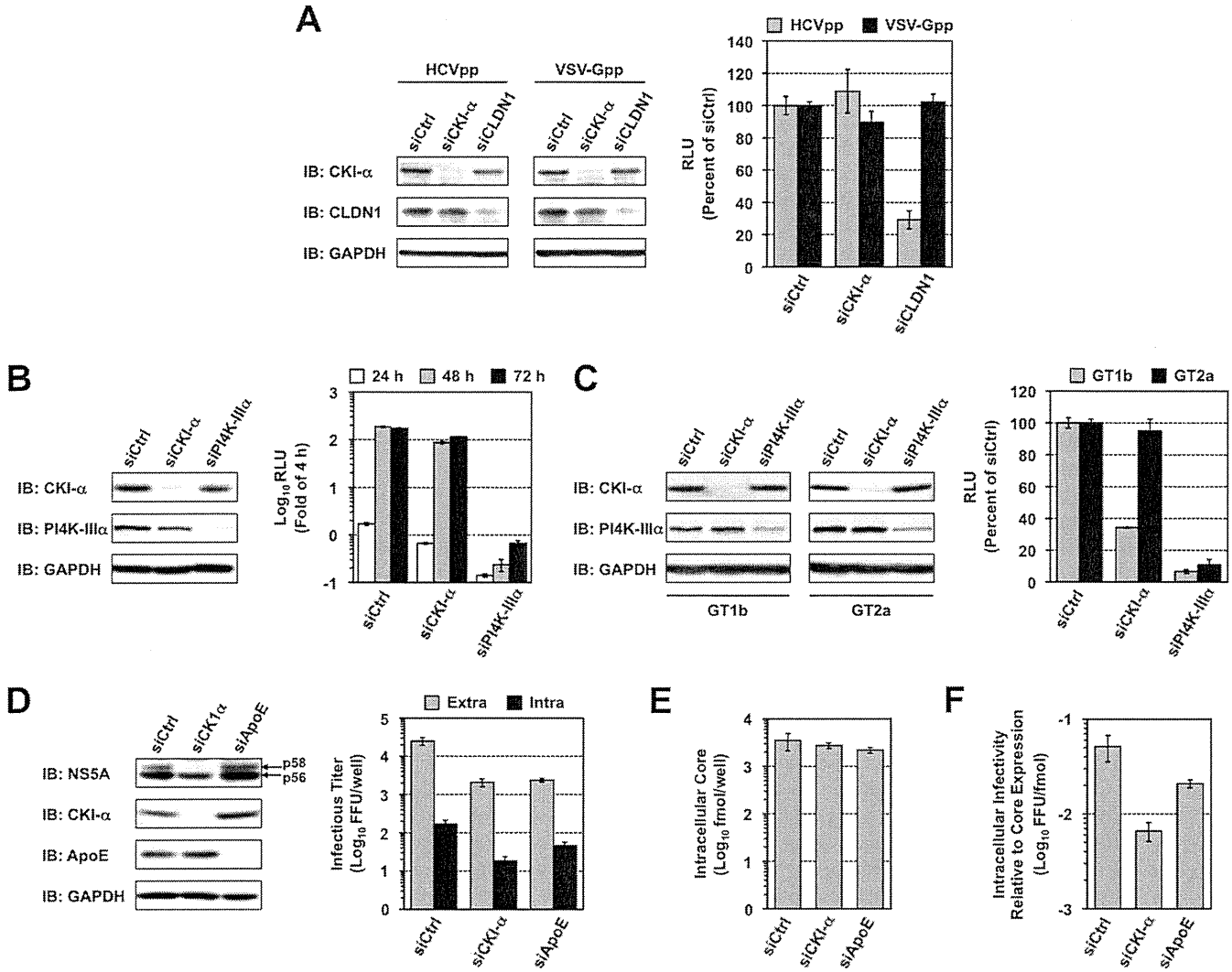


FIG 4 Virion assembly is a primary target of CKI-α. (A) Effect of CKI-α knockdown on viral entry. Huh7.5.1 cells were transfected with the indicated siRNAs. Two days later, cells were infected with HCVpp (gray bars) or VSV-Gpp (black bars) and harvested an additional 3 days later for immunoblotting (IB) and luciferase assays. Values were normalized to the value for transfection with control siRNAs (siCtrl), set at 100%. Values shown represent the means ± standard deviations from three independent transfections of siRNA. (B) Transient replication assay for the JFH-1 subgenomic replicon following CKI-α knockdown. Huh-7 cells transfected with the indicated siRNAs were coelectroporated with the identical siRNAs, and JFH-1 subgenomic luciferase reporter replicon RNA, and harvested at the indicated time points for immunoblotting (IB) and luciferase assays. The luciferase activity at each time point was corrected by the luciferase value at 4 h posttransfection to normalize transfection efficiencies. Values shown represent the means ± standard deviations from three replicate experiments. (C) Effects of CKI-α knockdown on replication in replicon cell lines derived from genotypes 1b and 2a. Two cell lines harboring an HCV subgenomic luciferase reporter replicon, LucNeo#2 (genotype 1b, GT1b) and SGR-JFH1/LucNeo (genotype 2a, GT2a), were transfected with the indicated siRNAs and harvested 3 days later for immunoblotting (IB) and luciferase assays. Luciferase activities were normalized to the luciferase values for transfection with control siRNA (siCtrl), set at 100%. Values shown represent the means ± standard deviations from three independent transfections of siRNA. (D) Effects of CKI-α knockdown on viral assembly and release. Huh7-25 cells transfected with the indicated siRNAs were coelectroporated with the identical siRNAs and JFH-1 RNA. Cells and supernatants were harvested 3 days later for immunoblotting (IB) and titrations of extracellular and intracellular infectious virus by focus-forming unit (FFU) assays. Values represent the means ± standard deviations from three replicate experiments. (E) Effect of CKI-α knockdown on the abundance of intracellular core protein. Amounts of core in cells for which results are shown in panel D were measured. Results represent the means ± standard deviations from three replicate experiments. (F) Effect of CKI-α knockdown on intracellular infectivity relative to core protein expression. Intracellular infectivity relative to core expression was determined by normalizing the yield of intracellular infectious virus (shown in panel D) with the amount of intracellular core protein shown in panel E. Results represent the means ± standard deviations from three replicate experiments.

followed by harvesting at different time points (Fig. 4B). The reporter luciferase activity at each time point was corrected with the luciferase value at 4 h posttransfection to normalize transfection efficiencies. Although efficient knockdown was achieved with siRNAs (Fig. 4B, left panel), CKI-α knockdown led to a marginal but nonnegligible decrease in the luciferase activity over the indicated time period. In contrast, PI4K-IIIα knockdown, as a positive control, resulted in a marked decrease (>200-fold) in activity (Fig. 4B, right panel). The effect of CKI-α silencing on the replication of the subgenomic replicon was further analyzed by using two cell lines derived from genotype 1b (LucNeo#2) (38, 39) and genotype 2a (SGR-JFH1/LucNeo) (Fig. 4C). Both Huh-7-based

subgenomic replicon cell lines carry a firefly luciferase reporter gene fused to the neomycin phosphotransferase gene. As shown in the right panel of Fig. 4C, knockdown of CKI-α resulted in a marked (~65%) decrease in replication of the genotype 1b replicon but only a slight (~10%) decrease in the genotype 2a replication, although knockdown efficiencies of CKI-α were sufficient and comparable in both cell lines (Fig. 4C, left panels). Our result with the genotype 1b replicon was consistent with a previous report (27). In contrast, the limited impact of CKI-α silencing on the replication of the JFH-1 subgenomic replicon suggests that the RNA replication step may not be a key role for CKI-α in the regulation of HCV JFH-1 production.

Finally, we focused on the late stages of the HCV life cycle and analyzed the involvement of CKI-α in virion assembly and release via a single-cycle virus production assay (55), in which Huh7–25 cells lacking CD81 expression were used. Three days posttransfection with siRNAs, the cells were cotransfected with the identical siRNAs and JFH-1 RNA by electroporation. The cells and culture supernatants were harvested after a further 3 days, and titrations of intra- and extracellular infectious virus were assessed (Fig. 4D to F). Reduced NS5A hyperphosphorylation was observed following CKI-α knockdown, but not following ApoE knockdown or transfection with irrelevant siRNA (Fig. 4D, left panel). Both CKI-α and ApoE knockdown led to an ~10-fold reduction in the yield of extracellular infectious virus compared to the negative control. Approximately a 9-fold reduction was found in the yield of intracellular infectious virus following CKI-α knockdown (Fig. 4D, right panel), indicating that CKI-α is not required for virus release from cells. Despite the marked decrease in intracellular virion yield, CKI-α knockdown resulted in only a 1.3-fold reduction in the abundance of intracellular core protein (Fig. 4E), supporting a limited impact for CKI-α knockdown on viral replication (Fig. 4B). Furthermore, CKI-α silencing led to approximately an 8-fold reduction in the intracellular infectivity relative to core protein expression, which represents the efficiency of viral assembly expressed as the yield of intracellular infectious virus normalized to the amount of intracellular core protein (Fig. 4F). Collectively, these observations suggest that in the HCV life cycle, CKI-α plays a key role most likely in the assembly of infectious viral particles.

**NS5A hyperphosphorylation mediated by CKI-α possibly contributes to recruitment of NS5A to low-density membrane structures around LDs in infected cells.** It has been demonstrated that recruitment of NS5A to cytoplasmic low-density membrane structures surrounding LDs, and the interaction of NS5A with the core protein at the site, are essential to HCV assembly (7, 8, 56). To gain mechanistic insight into the function of CKI-α in virion assembly, we performed a subcellular fractionation assay and examined whether NS5A phosphorylation by CKI-α contributed to the subcellular localization of NS5A. Lysates of cells transfected with JFH-1 RNA in the presence or absence of CKI-α silencing (Fig. 5A, left panel) were fractionated with 2.5 to 30% iodixanol gradients followed by immunoblotting of the fractions (Fig. 5A, right panels). In control cells (siCtrl), hyperphosphorylated p58 NS5A predominantly resided in low-density fractions, such as fractions 1 to 3, while hypophosphorylated p56 NS5A localized not only in the low-density fractions but also in high-density fractions, such as fractions 11 and 12. In contrast, knockdown of CKI-α (siCKI-α) decreased the abundance of hyperphosphorylated NS5A and NS5A in the low-density fractions. NS5A levels in the high-density fractions were not reduced by CKI-α knockdown. These results indicate that CKI-α is involved in the distribution of NS5A in cells as well as in its hyperphosphorylation.

We next assessed whether the intracellular localization of NS5A and its interaction with LDs or the core protein are affected by CKI-α knockdown by using laser-scanning confocal immunofluorescence microscopy. Cells were transfected either with CKI-α siRNA (siCKI-α) or with an irrelevant control siRNA (siCtrl), followed by infection with HCVcc. Efficient knockdown of CKI-α was confirmed by immunoblotting and was associated with decreased p58 expression (Fig. 5B). The delivery of siRNA into nearly 100% of the cells was observed with Cy3-labeled siRNA (Silencer Cy3-labeled GAPDH siRNA) (Fig. 5C). In siCtrl-transfected cells, NS5A was colocalized or closely associated with LDs. In contrast, its association with LDs was decreased following CKI-α depletion (Fig. 5D) ($P < 0.0001$ by two-sided Mann-Whitney test). Similarly, NS5A and the core protein were clearly colocalized in control cells, while their colocalization was reduced in CKI-α knockdown cells (Fig. 5E) ($P = 0.0110$ by two-sided Mann-Whitney test). These microscopy findings suggest that CKI-α and/or CKI-α-mediated hyperphosphorylation of NS5A is involved in the NS5A-core colocalization at or around LDs in HCV-infected cells. Taken together with the results of our subcellular fractionation assay (Fig. 5A), it is likely that CKI-α plays a role in recruiting NS5A to low-density membrane structures around LDs through hyperphosphorylation of NS5A, and it may facilitate the NS5A-core interaction at these sites.

**Identification of potential phospho-acceptor regions for CKI-α.** The above results prompted us to identify the phospho-acceptor sites for CKI-α by using a proteomics approach. Lysates of cells expressing the HCV JFH-1 genome, transfected with either CKI-α siRNA or an irrelevant control siRNA, were immunoprecipitated with an anti-NS5A antibody followed by SDS-PAGE (Fig. 6A). Immunoblotting showed a marked reduction of NS5A p58 following CKI-α knockdown (Fig. 6A, right panel). Silver-stained gel bands of p58 and p56 (Fig. 6A, left panel) were excised and subjected to in-gel digestion, followed by mass spectrometry analysis (Fig. 6B). A total of 629 peptides were identified from both control NS5A (siCtrl) and NS5A with CKI-α knockdown (siCKI-α) after peptide selection with a Mascot peptide score of ≥25 (see Table S3 in the supplemental material) and yielded 53% proteome coverage in total (49.4% for control NS5A and 41.8% for NS5A with CKI-α knockdown), as indicated in the upper panel of Fig. 6B (red letters). Peptides corresponding to domain III in NS5A were not obtained in this analysis. We identified three kinds of phosphopeptides (1, GSPPSEASSSVSQLSAPSLR; 2, AP TPPPR; 3, TVGLSESTISEALQQLAIK [Fig. 6B, upper panel, highlighted in green, blue, and yellow, respectively]) (see also Table S3). However, fine mapping of phosphorylation sites was not completely successful in this assay, probably due to the low abundance of immunoprecipitated NS5A. We next assessed which peptide contained the potential phospho-acceptor sites for CKI-α by comparing the frequencies of phosphopeptides identified with and without CKI-α knockdown. As shown in the lower panel of Fig. 6B, the frequency of phosphopeptide 1 relative to the total number of peptide 1 identified was decreased after CKI-α knockdown (from 26.2% to 19.8%). In contrast, the relative frequencies of phosphopeptides 2 and 3 were unaffected or increased by CKI-α knockdown. We noted that the threonine residue in peptide 2 is unlikely to be a consensus phosphorylation site of CKI

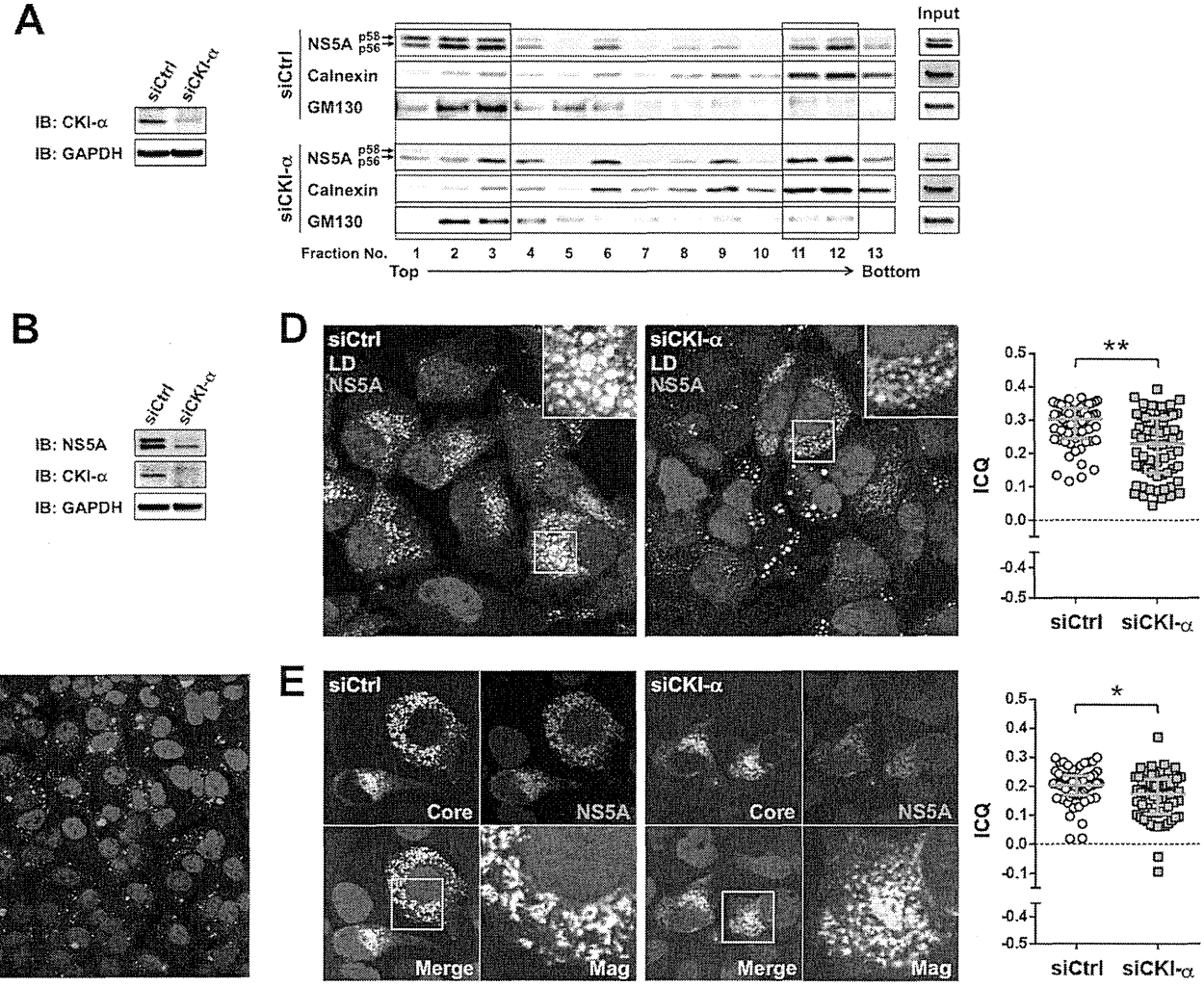


FIG 5 Effects of CKI-α knockdown on the subcellular localization of NS5A and its interaction with LDs or core protein. (A) Iodixanol density gradient analysis (right). Huh7-25 cells transfected with the indicated siRNAs were coelectroporated with the identical siRNAs and JFH-1 RNA. Cell lysates were prepared 3 days after electroporation and fractionated by iodixanol gradients of 2.5% to 30%. The gradient was collected in 0.8-ml fractions for immunoblotting. Total cell lysates before fractionation were loaded as input controls. Detected bands in fractions 1 to 3 and in fractions 11 and 12 are enclosed by squares. (Left) Immunoblotting (IB) results for CKI-α 3 days after electroporation. GAPDH was included as a loading control. (B) Immunoblot (IB) of NS5A and CKI-α 3 days after HCVcc infection. GAPDH was included as a loading control. (C) siRNA delivery efficiency. Cy3 fluorescence (red) was observed 3 days after transfection of Silencer Cy3-labeled GAPDH siRNA. Nuclei were counterstained with Hoechst 33342 (blue). (D) Colocalization of NS5A and LDs. Confocal microscopy images show cells transfected with either CKI-α siRNA (siCKI-α) or an irrelevant control siRNA (siCtrl), followed by infection with JFH-1 virus (left). Cells were fixed with paraformaldehyde 3 days after infection and labeled with an antibody specific for NS5A (red). Cells were counterstained with BODIPY 493/503 (green) to label lipid droplets and with Hoechst 33342 (blue) to label nuclei. Insets represent enlarged views of portions surrounded by squares. Colocalization of NS5A and LDs pixels were assessed quantitatively by intensity correlation analysis using ImageJ software (right). Plots shown represent the ICQ obtained from each of >60 NS5A/LD double-positive cells. Bars indicate the median ± interquartile range of the plots. **, $P < 0.01$ by two-sided Mann-Whitney test. (E) Colocalization of NS5A and core protein. Confocal microscopy images show cells transfected either with CKI-α siRNA (siCKI-α) or with a control siRNA (siCtrl), followed by infection with JFH-1 virus (left). Fixed cells were labeled with antibodies specific for NS5A (red) and core (green). Nuclei were counterstained with Hoechst 33342 (blue) in the merged images. Mag images represent enlarged views of portions surrounded by squares in the merged images. Colocalization of NS5A and core pixels was assessed quantitatively by intensity correlation analysis using ImageJ software (right). Plots shown represent ICQs obtained from each of >60 NS5A/core double-positive cells. Bars indicate the median ± interquartile range. *, $P < 0.05$ by two-sided Mann-Whitney test.

(57). Thus, the results suggest that peptide 1 (GSPPSEASSSVSQL SAPSLR) is the peptide most likely to contain the amino acids phosphorylated by CKI-α.

**S225 and S232 are key residues involved in NS5A hyperphosphorylation and hyperphosphorylation-dependent regulation of infectious virus production.** Peptide 1 identified above contains eight serine residues that are highly conserved among HCV isolates and are clustered within LCS I (Fig. 7A). To identify amino acids responsible for CKI-α-mediated hyperphosphorylation, we assessed the impacts of alanine or aspartic acid substitutions for these 8 serine residues on NS5A hyperphosphorylation and virus production. An HCV JFH-1 genome with the reporter luciferase, which enabled us to evaluate viral replication by measuring GLuc activity, and a series of its NS5A mutated constructs (Fig. 7A) were generated. Supernatants of cell cultures transfected with the RNA transcripts were harvested at 4, 24, 48, and 72 h posttransfection

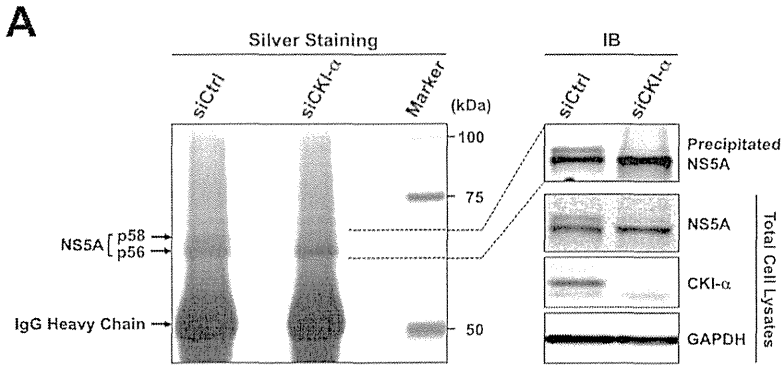


B

```
  1 SGSWLRDVWDWVCTILTDFKNWLTSKLFPKLPGLPFISCQ  40
 41 KGYKGVWAGTGIMTTRCPCGANISGNVRLGSMRITGPKTC  80
 81 MNTWQGTFPINCYTEGQCAPKPPTNYKTAIWRVAASEYAE 120
121 VTQHGSYSYVTGLTTDNLKIPCQLPSPEFFSWVDGVQIHR 160
161 FAPTPKPFFRDEVSFCVGLNSYAVGSQLPCEPEPDADVLR 200
201 SMLTDPPHITAETAARRLARGSPPSEASSSVSQLSAPSLR 240
241 ATCTTHSNTYDVDMVDANLLMEGGVAQTEPESRVPVLDFL 280
281 EPMAEEESDLEPSIPSECMLPRSGFPRALPAWARPDYNPP 320
321 LVESWRRPDYQPPTVAGCALPPPKRAPTPPPRRRRTVGLS 360
361 ESTISEALQQLAIKTFGQPPSSGDAGSSTGAGAAESGGPT 400
401 SPGEPAPSETGSASSMPPLEGEPGDPDLESDQVELQPPPQ 440
441 GGGVAPGSGSGSWSTCSEEDDTTVCC               466
```

| | Peptides Identified | No. of Peptides Identified Phospho/Total siCtrl | siCKI-α |
|---|---|---|---|
| #1 | GSPPSEASSS VSQLSAPSLR | 17/65 (26.2%) | 18/91 (19.8%) |
| #2 | APTPPPR | 16/28 (57.1%) | 14/21 (66.7%) |
| #3 | TVGLSESTIS EALQQLAIK | 1/16 (0.1%) | 1/14 (0.1%) |

FIG 6 Identification of NS5A phosphopeptides by a phospho-proteome approach. (A) Silver staining and immunoblotting of immunoprecipitated NS5A. Huh-7 cells transfected with the indicated siRNAs were coelectroporated with the identical siRNAs and JFH-1 RNA. Cell lysates were prepared 3 days after electroporation and immunoprecipitated with an anti-NS5A antibody. Immunoprecipitates were subjected to SDS-PAGE, followed by silver staining and immunoblotting (IB). (B) Phosphopeptide mapping of NS5A by LC-MS/MS analysis. p58 and p56 bands of NS5A were excised from the gel and subjected to in-gel digestion, followed by mass spectrometry analysis. Red letters represent the amino acids identified. Three kinds of phosphopeptides identified are highlighted in green (phosphopeptide 1), blue (phosphopeptide 2), and yellow (phosphopeptide 3). The numbers represent amino acid positions within NS5A.

and subjected to the GLuc assay. As shown in the left panel of Fig. 7B, serine-to-alanine substitution at either aa 229 (S229A) or at aa 235 (S235A) resulted in severe reduction in the viral replication. In contrast, the replication capacities of S222A, S228A, S230A, and S238A mutant reporter viruses were comparable to that of the wild type (WT). S225A and S232A mutations led to a slight but nonnegligible reduction in replication compared to WT. The phospho-mimetic aspartic acid substitution for aa 235 (S235D) exhibited a much higher replication capacity (~100-fold) than S235A, indicating that phosphorylation of S235 is required for efficient viral replication. In contrast, the replication capacity of S229D was still more-than-10-fold lower than that of WT, suggesting that introduction of negative charge at this position is not sufficient to enhance viral replication (Fig. 7B, right panel). S225D and S232D mutations restored viral replication capacities and exhibited the same replication phenotype as WT. Interestingly, S222D and S230D resulted in a slight reduction in viral replication compared to S222A and S230A, consistent with previous reports (23, 58) (Fig. 7B, right panel).

We next evaluated the effects of the NS5A mutations on infectious virus production by titrations of infectious virus in culture supernatants of cells transfected with RNA transcripts of JFH-1 viruses at 72 h posttransfection (Fig. 7C). S225A and S232A mutations resulted in 4- and 5-fold reductions in the virus infectious titer, respectively, compared to WT, while the abilities of S225D and S232D mutants to produce infectious virus were comparable to that of WT. Little or no virus production was observed with S229A, S229D, and S235A mutations, presumably because of their strong negative impacts on viral replication. A slight reduction in virus production observed with S230D and S235D mutations was most likely due to their replication capacities. S222A, S222D, S228A, S228D, S230A, S238A, and S238D substitutions had no significant effect on virus production (>75% of the WT level).

To determine the effect of the NS5A mutations on NS5A hyperphosphorylation, cells expressing JFH-1 viruses were subjected to immunoblotting, and the p58/p56 ratio of NS5A was estimated (Fig. 7D). The hyperphosphorylated p58 band of NS5A was clearly detected in cells transfected with WT and S222A, S228A, S230A, and S238A mutants, which had mean p58/p56 ratios of 0.42, 0.38, 0.35, 0.50, and 0.60, respectively. These p58/p56 ratios were reproducible in multiple repeated experiments but much lower than the p58/p56 ratios (e.g., 0.93 in siCtrl-transfected cells) in Fig. 3A. This difference may be attributed to the difference in the way by which HCV was introduced into cells (virus infection in Fig. 3A and transfection of viral genome in Fig. 7D and F). The p58 levels were significantly reduced in cells transfected with S225A or S232A mutants, which had mean p58/p56 ratios of 0.11 and 0.15, respectively (Fig. 7D). Since the p58/p56 ratios of the S229A and S235A mutants were not determined due to low levels of NS5A expression, we reevaluated the p58/p56 ratio of each viral muatant by using a vaccinia virus-T7 polymerase-mediated protein expression system (Fig. 7E, left panel). Cells transfected with pJFH1 or a series of its NS5A mutants were infected with vaccinia virus expressing the T7 RNA polymerase and harvested for immunoblotting. Similar to the results shown in Fig. 7D, the p58/p56 ratios of S225A and S232A mutants were significantly reduced, while S229A and S235A mutations had no effects (Fig. 7E, right panel). The hyperphosphorylated band of NS5A was observed in cells transfected with the S222D, S225D, S228D, S229D, or S230D mutant in both experimental settings. Interestingly, the S232D, S235D, and S238D mutations resulted in a slight retardation of p56 mobility (Fig. 7F and G), consistent with previous reports (58, 59).

Collectively, S225 and S232 are key residues involved in

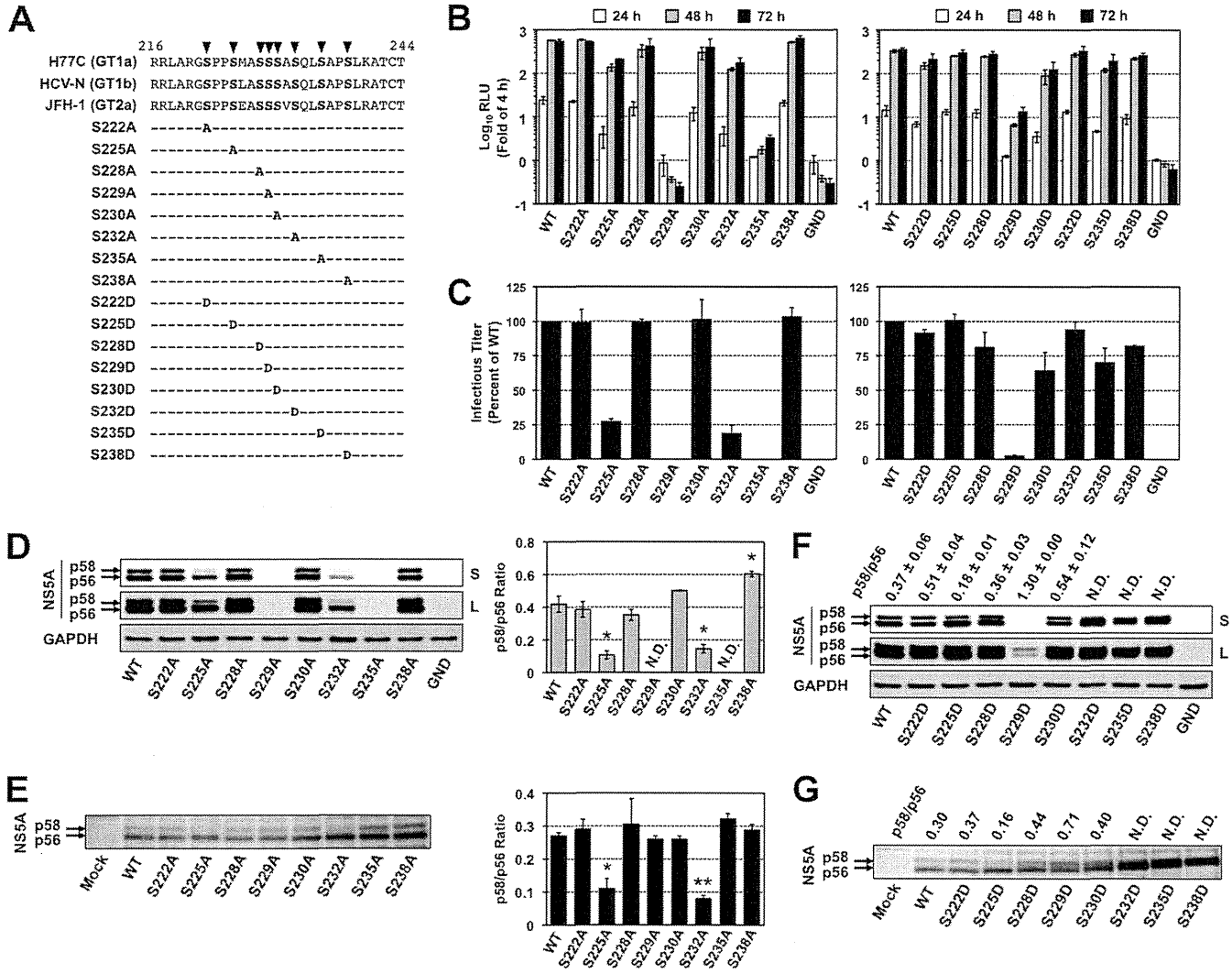


FIG 7 Effects of mutations at potential CKI-α phosphorylation sites on NS5A hyperphosphorylation, viral replication, and infectious virion production. (A) Highly conserved serine residues located within the LCS I region of NS5A and the sequences of NS5A mutants used. Arrowheads represent putative phosphorylation sites replaced with alanine or aspartic acid. The numbers represent amino acid positions within NS5A. (B) Viral replication. Huh-7 cells were transfected with the indicated JFH-1-based GLuc reporter constructs, including the WT and its replication-defective mutant (GND). Culture supernatants were harvested at the indicated time points for luciferase assays. The GLuc activity at each time point was normalized with the activity at 4 h posttransfection, and the fold chnages are shown. Results represent the means ± standard deviations from three independent experiments, each performed in triplicate. (C) Infectious virion production. Huh-7 cells were transfected with the indicated JFH-1 viral RNAs, including the WT and its replication-defective mutant (GND). Culture supernatants were harvested 3 days (72 h) later for titrations of infectious virus in a focus-forming unit (FFU) assay. The infectious virus yield of each NS5A mutant was normalized with that of JFH-1 WT, which was set at 100%. Results represent the means ± standard deviations from multiple independent experiments, each performed at least in triplicate. (D) Immunoblot of NS5A in lysates of cells transfected with JFH-1 viral RNAs carrying the indicated serine-to-alanine mutations (left). GAPDH is a loading control. The p58/p56 ratio of each virus was determined by carrying out densitometric analysis of NS5A bands (right). Results shown represent the means ± standard deviations from multiple independent experiments. *, $P < 0.05$, compared to WT. N.D., not determined, due to low levels of expression. (E) Vaccinia virus-T7 polymerase-mediated expression of NS5A in cells transfected with pJFH1 carrying the indicated serine-to-alanine mutations (left). NS5A bands were quantified by densitometric analysis, and p58/p56 ratios were calculated (right). Data shown represent the means ± standard deviations from multiple independent experiments. *, $P < 0.05$; **, $P < 0.01$ (versus WT). (F) Immunoblot of NS5A in lysates of cells transfected with JFH-1 viral RNA carrying the indicated serine-to-aspartic acid mutation. GAPDH was included as a loading control. The p58/p56 ratio of each virus was determined by carrying out densitometric analysis of NS5A bands. Results shown represent the means ± standard deviations from multiple independent experiments. N.D., not determined, due to the poor separation of p58 and p56 bands. (G) Vaccinia virus-T7 polymerase-mediated expression of NS5A in cells transfected with pJFH1 carrying the indicated serine-to-aspartic acid mutation. NS5A bands were quantified by densitometric analysis, and p58/p56 ratios were calculated. Data shown are representative of two independent experiments. N.D., not determined, due to the poor separation of p58 and p56 bands. S and L in panels D and F represent short exposure and long exposure, respectively.

NS5A hyperphosphorylation and hyperphosphorylation-dependent regulation of infectious virus production. In addition, S225A and S232A reproduced the viral phenotype following CKI-α knockdown more precisely than the other serine mutants within the peptide 1 region. It is most likely that S225 and S232 of NS5A are important for CKI-α-mediated hyperphosphorylation, which is involved in the robust production of infectious HCV.

## DISCUSSION

Phosphorylation at serine and threonine residues in HCV NS5A is critical for regulation of the viral life cycle, including genome replication and infectious virus assembly (8, 9, 14, 16–18, 59–61). Several serine/threonine protein kinases have been identified as enzymes that potentially phosphorylate NS5A (9, 25, 26, 28, 50, 51). To our knowledge, however, this study is the first to identify through a kinome-wide screening protein kinases that interact with and phosphorylate NS5A. The *in vitro* AlphaScreen and phosphorylation assays, followed by RNAi screening on the HCVcc system, identified CKI-α as a major NS5A-associated kinase involved in NS5A hyperphosphorylation and the production of infectious virus.

In a previous study, CKI-α was reported to be involved in the replication of the subgenomic replicon derived from genotype 1b, with evidence that attenuation of CKI-α expression inhibited viral RNA replication up to 60% 5 days after the CKI-α knockdown (27). However, our study with the HCVcc system, as well as detailed analyses dissecting individual steps in the HCV life cycle, revealed that virion assembly is more affected by CKI-α silencing than is viral genome replication. It is highly likely that the CKI-α-mediated hyperphosphorylation of NS5A plays a role in recruiting NS5A to low-density membrane structures around LDs, leading to the acceleration of the early step(s) of virus particle formation. Mutagenesis analyses of putative CKI-α phosphorylation sites identified by a phospho-proteomic approach demonstrated that serine-to-alanine substitution at aa 225 or aa 232 in NS5A did to some extent reproduce the viral phenotype following CKI-α knockdown, indicating that S225 and S232 may be key residues for CKI-α-mediated NS5A hyperphosphorylation and regulation of virion assembly.

It is commonly held that HCV replication is regulated through the tight and delicate control of the ratio between p58 and p56 levels. Adaptive mutations or kinase inhibitors, which reduce NS5A hyperphosphorylation, enhance the HCV RNA replication of genotype 1 isolates, possibly by modulating its interaction with the host vesicle-associated membrane protein-associated protein subtype A (VAP-A), which is an essential factor for HCV replication (17–19, 24). In contrast, reduction of NS5A hyperphosphorylation by RNAi targeting protein kinases results in inhibition of the replication of genotype 1 adaptive replicons, indicating a role for p58 in efficient viral replication (25, 27). Impaired RNA replication resulting from reduced NS5A hyperphosphorylation has also been reported in the case of JFH-1 or JFH-1-based recombinant virus (25, 58–60). Consistent with a previous report (27), we found that CKI-α depletion inhibited the replication of the genotype 1b subgenomic replicon LucNeo#2, which carries the adaptive S2204R mutation in NS5A (38, 39) (Fig. 4C). Our transient-replication assay with the JFH-1 subgenomic replicon showed a slight but significant reduction in replication following CKI-α depletion (Fig. 4B). However, CKI-α silencing did not affect RNA replication in SGR-JFH1/LucNeo cells, where the JFH-1 subgenomic replicon stably replicates (Fig. 4C). Thus, the involvement of CKI-α in HCV RNA replication might be genotype or isolate dependent. We observed a difference in the replication capacity following CKI-α knockdown between transient and stable replication of JFH-1 replicons (Fig. 4B and C). A moderate reduction of replication was also detected when the JFH-1 genome carrying the S225A or S232A mutation was transiently transfected (Fig. 7B). One may infer that CKI-α is involved in the initiation of viral RNA replication rather than in its maintenance.

Our intra- and extracellular infectivity assays following CKI-α depletion suggested that CKI-α primarily targets virion assembly in the HCV life cycle (Fig. 4D to F), although a slight but nonnegligible negative effect of CKI-α knockdown on viral replication was observed (Fig. 4B). It is accepted that the assembly of HCV particles requires recruitment of NS proteins, including NS5A as well as structural proteins, to cytoplasmic membrane structures around LDs, leading to an interaction between NS5A and the core, which is important for efficient encapsidation of the viral genome (7, 8, 56). To understand how CKI-α is involved in virion assembly, we performed a subcellular fractionation assay and immunofluorescence confocal microscopy. Our subcellular fractionation assay clearly showed that hyperphosphorylated NS5A, p58, is mainly localized in low-density membrane fractions, while hypophosphorylated NS5A, p56, prefers high-density fractions. NS5A abundance in lighter fractions was decreased following CKI-α depletion (Fig. 5A). These results are supported by microscopic analyses that demonstrated that CKI-α silencing reduced colocalization of NS5A with LDs and the core (Fig. 5D and E). We tried to confirm the interaction of NS5A and core in HCVcc-infected cells that had been transfected with CKI-α siRNA or irrelevant siRNA. However, the interaction was not observed under this condition, presumably because immunoprecipitated NS5A and/or core was not abundant enough to assess their coimmunoprecipitation in siRNA-transfected cells. Alternatively, we assessed the interaction in Huh-7 cells coexpressing core and NS5A, although no p58 form (no functional NS5A) was detected in this setting. We clearly detected the interaction of NS5A and core in this experiment and found that CKI-α depletion had no significant effect on this interaction (data not shown). Taken together with the results of confocal microscopy (Fig. 5E), this finding might suggest that both (i) phosphorylation of serine residues in the C terminus of NS5A, which is involved in the generation of basally phosphorylated NS5A, as shown previously (8), and (ii) CKI-α-mediated hyperphosphorylation, in which serine residues in the LCS I region are mainly involved, are important for an efficient interaction between NS5A and core in HCV replicating cells. Collectively, CKI-α-mediated hyperphosphorylation of NS5A may contribute to an increase in the local concentration of NS5A at low-density membrane structures around LDs rather than in facilitating the physical interaction of NS5A and core. The relationship between the phosphorylation status of NS5A and its localization on cellular membranes has been previously reported. Miyanari et al. showed that mutated NS5A expressed from JFH-1 variants (JFH1$^{AAA99}$ and JFH1$^{AAA102}$ in their report), whose p58/p56 ratios were lower than that of wild-type virus, was not recruited to LDs (56). Qiu et al. fractionated lysates from replicon cells and demonstrated that a substantial amount of hyperphosphorylated NS5A was detected in lighter fractions. Treatment with an NS5A inhibitor, BMS-790052, reduced hyperphosphorylation of NS5A and concomitantly decreased the overall amount of NS5A in low-density membrane fractions (62). These findings raise questions about the regulatory mechanism(s) of the subcellular localization of NS5A, especially at low-density membrane structures. The above-mentioned NS5A mutants, JFH1$^{AAA99}$ and JFH1$^{AAA102}$, have triple alanine substitutions for the APK sequence at aa 99 to 101 and the PPT sequence at aa 102 to 104 in NS5A, respectively, but neither is likely to be a CKI recognition site. In addition, the NS5A inhibitor

has no inhibitory effect on CKI activity (62). Thus, it appears that two or more kinds of serine/threonine-specific protein kinases, including CKI-α, participate in NS5A phosphorylation that is important for the regulation of its subcellular distribution. It is tempting to speculate that host factors involved in membrane trafficking or lipogenesis possibly interact with NS5A in a phosphorylation-dependent manner and facilitate recruitment of NS5A to low-density membrane structures surrounding LDs. Although further study is needed to validate this speculation, NS5A-interacting factors, such as VAP-A and diacylglycerol acyltransferase-1 (19, 63, 64), might be candidates for involvement in the regulation of this process.

To identify potential phospho-acceptor sites for CKI-α, a phospho-proteome analysis was carried out with NS5A isolated from HCVcc-infected cell lines with and without CKI-α knockdown (Fig. 6). Three kinds of phosphopeptides were identified out of a total of 629 peptides after peptide selection, although fine mapping of the phosphorylation sites was not completely successful. Among them, only the relative frequency of phosphopeptide 1 (GSPPSEASSSVSQLSAPSLR) was decreased after CKI-α knockdown, suggesting the possibility that peptide 1 contains amino acids phosphorylated by CKI-α. Serine residues in peptide 1, which are well conserved among HCV genotypes, matched the consensus sequences for CKI-α-mediated phosphorylation (57). In contrast, a threonine residue in peptide 2 is not conserved and does not match the consensus sequences for phosphorylation by CKI-α. The frequency of phosphopeptide 3 was unchanged with and without CKI-α knockdown (0.1% versus 0.1%). Further mutagenesis analyses targeting the peptide 1 region suggested that S225 and S232 are possible CKI-α phosphorylation sites involved in NS5A hyperphosphorylation and infectious virus production, because alanine substitution for either of these serine residues reproduced the viral phenotype after CKI-α knockdown more accurately than the other mutants within the peptide 1 region (Fig. 7B to E). The S229A and S235A mutations severely impaired viral replication, suggesting that phosphorylation at S229 and S235 is essential for efficient viral replication (Fig. 7B). However, the HCV protein expression assay using vaccinia virus expressing the T7 RNA polymerase revealed that phosphorylation of these residues is not involved in NS5A hyperphosphorylation (Fig. 7E). In the case of genotype 1 isolates, NS5A mutations that reduce hyperphosphorylation enhanced viral RNA replication (17, 18). However, this was not the case for the S225A or S232A mutation in genotype 2a. In addition, S229A and S235A mutations in genotype 1b (Con1) markedly enhance viral replication (18), but the same mutations are lethal in genotype 2a. S232 has been shown to be a potential phosphorylation site for CKI-α by a peptide-based kinase assay *in vitro* (28). However, the present study is the first to demonstrate the significance of phosphorylation at S225 and S232 in infectious virus production. The sequence coverage of NS5A by our mass spectrometry analysis was less than 60% and was especially low in domain III of NS5A (Fig. 6B). We cannot exclude the possibility of the presence of additional CKI-α phosphorylation sites in NS5A.

Recently, two cellular kinases involved in the regulation of NS5A phosphorylation have been identified. PI4K-IIIα is essential for HCV replication (65–70) and catalyzes the synthesis of phosphatidylinositol 4-phosphate accumulating in HCV replicating cells through its enzymatic activation resulting from an interaction with NS5A (71, 72). PI4K-IIIα directly interacts with the C-terminal end of NS5A domain I, and NS5A–PI4K-IIIα binding is essential for viral replication. Its depletion resulted in a relative increase of p58 abundance, while overexpression of enzymatically active PI4K-IIIα increased the relative abundance of p56 (73). Plk1 has been shown to play a role in viral replication through hyperphosphorylation of NS5A (25). Plk1 was coimmunoprecipitated with NS5A, and knockdown of Plk1 or treatment with a specific inhibitor decreased both NS5A hyperphosphorylation and HCV replication. Since the recognition sites for CKI-α, PI4K-IIIα, and Plk1 have been assumed to be spatially close to each other (25, 28, 73), it is interesting to analyze their interactive actions in regard to regulation of NS5A phosphorylation.

The exquisite balance between the two different phosphorylated forms of NS5A has been proposed to regulate the HCV life cycle; basally phosphorylated p56 abundance is hypothetically involved in viral RNA replication, and hyperphosphorylated p58 is required for virion assembly (9, 17, 18, 73, 74). However, this hypothesis has not yet been fully proven. Our results here provide strong evidence supporting the involvement of NS5A hyperphosphorylation in viral assembly and that of CKI-α in mediating this process. These results not only contribute to a better understanding of the regulatory details of the HCV life cycle but also illuminate targets for potential antiviral strategies.

## ACKNOWLEDGMENTS

We are grateful to F. V. Chisari for kindly providing Huh7.5.1 cells, C. M. Rice for providing anti-NS5A mouse monoclonal antibody (9E10), K. Watashi and K. Shimotohno for providing LucNeo#2 cells, T. Pietschmann for providing the expression plasmid carrying the JFH-1 envelope glycoprotein gene, and Y. Matsuura for providing the plasmid expressing the VSV-G envelope glycoprotein. We thank D. Akazawa for help in preparing HCVpp, the Michael Hooker Microscopy Facility of the University of North Carolina for assistance with confocal microscopy, M. Sasaki, N. Sugiyama, K. Goto, and T. Date for their technical assistance, and T. Mizoguchi for secretarial assistance.

This work was supported in part by grants-in-aid from the Ministry of Health, Labor, and Welfare of Japan and the Ministry of Education, Culture, Sports, Science, and Technology, Japan, by Research on Health Sciences Focusing on Drug Innovation from the Japan Health Sciences Foundation, and by a grant (R01-AI095690) from the U.S. National Institutes of Health.

## REFERENCES

1. **Shepard CW, Finelli L, Alter MJ.** 2005. Global epidemiology of hepatitis C virus infection. Lancet Infect. Dis. 5:558–567. http://dx.doi.org/10.1016/S1473-3099(05)70216-4.
2. **Alter MJ.** 2007. Epidemiology of hepatitis C virus infection. World J. Gastroenterol. 13:2436–2441. http://www.wjgnet.com/1007-9327/13/2436.asp.
3. **Choo QL, Richman KH, Han JH, Berger K, Lee C, Dong C, Gallegos C, Coit D, Medina-Selby R, Barr PJ, Weiner AJ, Bradley DW, Kuo G, Houghton M.** 1991. Genetic organization and diversity of the hepatitis C virus. Proc. Natl. Acad. Sci. U. S. A. 88:2451–2455. http://dx.doi.org/10.1073/pnas.88.6.2451.
4. **Suzuki T, Ishii K, Aizaki H, Wakita T.** 2007. Hepatitis C viral life cycle. Adv. Drug Deliv. Rev. 59:1200–1212. http://dx.doi.org/10.1016/j.addr.2007.04.014.
5. **Lohmann V, Korner F, Koch J, Herian U, Theilmann L, Bartenschlager R.** 1999. Replication of subgenomic hepatitis C virus RNAs in a hepatoma cell line. Science 285:110–113. http://dx.doi.org/10.1126/science.285.5424.110.
6. **Egger D, Wolk B, Gosert R, Bianchi L, Blum HE, Moradpour D, Bienz K.** 2002. Expression of hepatitis C virus proteins induces distinct membrane alterations including a candidate viral replication complex. J. Virol. 76:5974–5984. http://dx.doi.org/10.1128/JVI.76.12.5974-5984.2002.

7. Appel N, Zayas M, Miller S, Krijnse-Locker J, Schaller T, Friebe P, Kallis S, Engel U, Bartenschlager R. 2008. Essential role of domain III of nonstructural protein 5A for hepatitis C virus infectious particle assembly. PLoS Pathog. 4:e1000035. http://dx.doi.org/10.1371/journal.ppat.1000035.
8. Masaki T, Suzuki R, Murakami K, Aizaki H, Ishii K, Murayama A, Date T, Matsuura Y, Miyamura T, Wakita T, Suzuki T. 2008. Interaction of hepatitis C virus nonstructural protein 5A with core protein is critical for the production of infectious virus particles. J. Virol. 82:7964–7976. http://dx.doi.org/10.1128/JVI.00826-08.
9. Tellinghuisen TL, Foss KL, Treadaway J. 2008. Regulation of hepatitis C virion production via phosphorylation of the NS5A protein. PLoS Pathog. 4:e1000032. http://dx.doi.org/10.1371/journal.ppat.1000032.
10. Shi ST, Lee KJ, Aizaki H, Hwang SB, Lai MM. 2003. Hepatitis C virus RNA replication occurs on a detergent-resistant membrane that cofractionates with caveolin-2. J. Virol. 77:4160–4168. http://dx.doi.org/10.1128/JVI.77.7.4160-4168.2003.
11. Miyanari Y, Hijikata M, Yamaji M, Hosaka M, Takahashi H, Shimotohno K. 2003. Hepatitis C virus non-structural proteins in the probable membranous compartment function in viral genome replication. J. Biol. Chem. 278:50301–50308. http://dx.doi.org/10.1074/jbc.M305684200.
12. Tellinghuisen TL, Marcotrigiano J, Rice CM. 2005. Structure of the zinc-binding domain of an essential component of the hepatitis C virus replicase. Nature 435:374–379. http://dx.doi.org/10.1038/nature03580.
13. Huang L, Hwang J, Sharma SD, Hargittai MR, Chen Y, Arnold JJ, Raney KD, Cameron CE. 2005. Hepatitis C virus nonstructural protein 5A (NS5A) is an RNA-binding protein. J. Biol. Chem. 280:36417–36428. http://dx.doi.org/10.1074/jbc.M508175200.
14. Reed KE, Xu J, Rice CM. 1997. Phosphorylation of the hepatitis C virus NS5A protein in vitro and in vivo: properties of the NS5A-associated kinase. J. Virol. 71:7187–7197.
15. Tanji Y, Kaneko T, Satoh S, Shimotohno K. 1995. Phosphorylation of hepatitis C virus-encoded nonstructural protein NS5A. J. Virol. 69:3980–3986.
16. Kaneko T, Tanji Y, Satoh S, Hijikata M, Asabe S, Kimura K, Shimotohno K. 1994. Production of two phosphoproteins from the NS5A region of the hepatitis C viral genome. Biochem. Biophys. Res. Commun. 205:320–326. http://dx.doi.org/10.1006/bbrc.1994.2667.
17. Blight KJ, Kolykhalov AA, Rice CM. 2000. Efficient initiation of HCV RNA replication in cell culture. Science 290:1972–1974. http://dx.doi.org/10.1126/science.290.5498.1972.
18. Appel N, Pietschmann T, Bartenschlager R. 2005. Mutational analysis of hepatitis C virus nonstructural protein 5A: potential role of differential phosphorylation in RNA replication and identification of a genetically flexible domain. J. Virol. 79:3187–3194. http://dx.doi.org/10.1128/JVI.79.5.3187-3194.2005.
19. Evans MJ, Rice CM, Goff SP. 2004. Phosphorylation of hepatitis C virus nonstructural protein 5A modulates its protein interactions and viral RNA replication. Proc. Natl. Acad. Sci. U. S. A. 101:13038–13043. http://dx.doi.org/10.1073/pnas.0405152101.
20. Katze MG, Kwieciszewski B, Goodlett DR, Blakely CM, Neddermann P, Tan SL, Aebersold R. 2000. Ser(2194) is a highly conserved major phosphorylation site of the hepatitis C virus nonstructural protein NS5A. Virology 278:501–513. http://dx.doi.org/10.1006/viro.2000.0662.
21. Reed KE, Rice CM. 1999. Identification of the major phosphorylation site of the hepatitis C virus H strain NS5A protein as serine 2321. J. Biol. Chem. 274:28011–28018.
22. Nordle Gilliver A, Griffin S, Harris M. 2010. Identification of a novel phosphorylation site in hepatitis C virus NS5A. J. Gen. Virol. 91:2428–2432. http://dx.doi.org/10.1099/vir.0.023614-0.
23. Lemay KL, Treadaway J, Angulo I, Tellinghuisen TL. 2013. A hepatitis C virus NS5A phosphorylation site that regulates RNA replication. J. Virol. 87:1255–1260. http://dx.doi.org/10.1128/JVI.02154-12.
24. Neddermann P, Quintavalle M, Di Pietro C, Clementi A, Cerretani M, Altamura S, Bartholomew L, De Francesco R. 2004. Reduction of hepatitis C virus NS5A hyperphosphorylation by selective inhibition of cellular kinases activates viral RNA replication in cell culture. J. Virol. 78:13306–13314. http://dx.doi.org/10.1128/JVI.78.23.13306-13314.2004.
25. Chen YC, Su WC, Huang JY, Chao TC, Jeng KS, Machida K, Lai MM. 2010. Polo-like kinase 1 is involved in hepatitis C virus replication by hyperphosphorylating NS5A. J. Virol. 84:7983–7993. http://dx.doi.org/10.1128/JVI.00068-10.
26. Coito C, Diamond DL, Neddermann P, Korth MJ, Katze MG. 2004. High-throughput screening of the yeast kinome: identification of human serine/threonine protein kinases that phosphorylate the hepatitis C virus NS5A protein. J. Virol. 78:3502–3513. http://dx.doi.org/10.1128/JVI.78.7.3502-3513.2004.
27. Quintavalle M, Sambucini S, Di Pietro C, De Francesco R, Neddermann P. 2006. The alpha isoform of protein kinase CKI is responsible for hepatitis C virus NS5A hyperphosphorylation. J. Virol. 80:11305–11312. http://dx.doi.org/10.1128/JVI.01465-06.
28. Quintavalle M, Sambucini S, Summa V, Orsatti L, Talamo F, De Francesco R, Neddermann P. 2007. Hepatitis C virus NS5A is a direct substrate of casein kinase I-alpha, a cellular kinase identified by inhibitor affinity chromatography using specific NS5A hyperphosphorylation inhibitors. J. Biol. Chem. 282:5536–5544. http://dx.doi.org/10.1074/jbc.M610486200.
29. Kato T, Date T, Miyamoto M, Sugiyama M, Tanaka Y, Orito E, Ohno T, Sugihara K, Hasegawa I, Fujiwara K, Ito K, Ozasa A, Mizokami M, Wakita T. 2005. Detection of anti-hepatitis C virus effects of interferon and ribavirin by a sensitive replicon system. J. Clin. Microbiol. 43:5679–5684. http://dx.doi.org/10.1128/JCM.43.11.5679-5684.2005.
30. Wakita T, Pietschmann T, Kato T, Date T, Miyamoto M, Zhao Z, Murthy K, Habermann A, Krausslich HG, Mizokami M, Bartenschlager R, Liang TJ. 2005. Production of infectious hepatitis C virus in tissue culture from a cloned viral genome. Nat. Med. 11:791–796. http://dx.doi.org/10.1038/nm1268.
31. Phan T, Beran RK, Peters C, Lorenz IC, Lindenbach BD. 2009. Hepatitis C virus NS2 protein contributes to virus particle assembly via opposing epistatic interactions with the E1–E2 glycoprotein and NS3-NS4A enzyme complexes. J. Virol. 83:8379–8395. http://dx.doi.org/10.1128/JVI.00891-09.
32. Tannous BA, Kim DE, Fernandez JL, Weissleder R, Breakefield XO. 2005. Codon-optimized Gaussia luciferase cDNA for mammalian gene expression in culture and in vivo. Mol. Ther. 11:435–443. http://dx.doi.org/10.1016/j.ymthe.2004.10.016.
33. Ryan MD, King AM, Thomas GP. 1991. Cleavage of foot-and-mouth disease virus polyprotein is mediated by residues located within a 19 amino acid sequence. J. Gen. Virol. 72:2727–2732. http://dx.doi.org/10.1099/0022-1317-72-11-2727.
34. Niwa H, Yamamura K, Miyazaki J. 1991. Efficient selection for high-expression transfectants with a novel eukaryotic vector. Gene 108:193–199. http://dx.doi.org/10.1016/0378-1119(91)90434-D.
35. Zhong J, Gastaminza P, Cheng G, Kapadia S, Kato T, Burton DR, Wieland SF, Uprichard SL, Wakita T, Chisari FV. 2005. Robust hepatitis C virus infection in vitro. Proc. Natl. Acad. Sci. U. S. A. 102:9294–9299. http://dx.doi.org/10.1073/pnas.0503596102.
36. Akazawa D, Date T, Morikawa K, Murayama A, Miyamoto M, Kaga M, Barth H, Baumert TF, Dubuisson J, Wakita T. 2007. CD81 expression is important for the permissiveness of Huh7 cell clones for heterogeneous hepatitis C virus infection. J. Virol. 81:5036–5045. http://dx.doi.org/10.1128/JVI.01573-06.
37. Kato T, Date T, Miyamoto M, Furusaka A, Tokushige K, Mizokami M, Wakita T. 2003. Efficient replication of the genotype 2a hepatitis C virus subgenomic replicon. Gastroenterology 125:1808–1817. http://dx.doi.org/10.1053/j.gastro.2003.09.023.
38. Murata T, Ohshima T, Yamaji M, Hosaka M, Miyanari Y, Hijikata M, Shimotohno K. 2005. Suppression of hepatitis C virus replicon by TGF-beta. Virology 331:407–417. http://dx.doi.org/10.1016/j.virol.2004.10.036.
39. Goto K, Watashi K, Murata T, Hishiki T, Hijikata M, Shimotohno K. 2006. Evaluation of the anti-hepatitis C virus effects of cyclophilin inhibitors, cyclosporin A, and NIM811. Biochem. Biophys. Res. Commun. 343:879–884. http://dx.doi.org/10.1016/j.bbrc.2006.03.059.
40. Murayama A, Sugiyama N, Yoshimura S, Ishihara-Sugano M, Masaki T, Kim S, Wakita T, Mishiro S, Kato T. 2012. A subclone of HuH-7 with enhanced intracellular hepatitis C virus production and evasion of virus related-cell cycle arrest. PLoS One 7:e52697. http://dx.doi.org/10.1371/journal.pone.0052697.
41. Tadokoro D, Takahama S, Shimizu K, Hayashi S, Endo Y, Sawasaki T. 2010. Characterization of a caspase-3-substrate kinome using an N- and C-terminally tagged protein kinase library produced by a cell-free system. Cell Death Dis. 1:e89. http://dx.doi.org/10.1038/cddis.2010.65.
42. Sawasaki T, Gouda MD, Kawasaki T, Tsuboi T, Tozawa Y, Takai K, Endo Y. 2005. The wheat germ cell-free expression system: methods for high-throughput materialization of genetic information. Methods Mol. Biol. 310:131–144. http://dx.doi.org/10.1007/978-1-59259-948-6_10.
43. Sawasaki T, Ogasawara T, Morishita R, Endo Y. 2002. A cell-free protein

synthesis system for high-throughput proteomics. Proc. Natl. Acad. Sci. U. S. A. 99:14652–14657. http://dx.doi.org/10.1073/pnas.232580399.
44. Sawasaki T, Kamura N, Matsunaga S, Saeki M, Tsuchimochi M, Morishita R, Endo Y. 2008. Arabidopsis HY5 protein functions as a DNA-binding tag for purification and functional immobilization of proteins on agarose/DNA microplate. FEBS Lett. 582:221–228. http://dx.doi.org/10.1016/j.febslet.2007.12.004.
45. Bartosch B, Dubuisson J, Cosset FL. 2003. Infectious hepatitis C virus pseudo-particles containing functional E1–E2 envelope protein complexes. J. Exp. Med. 197:633–642. http://dx.doi.org/10.1084/jem.20021756.
46. Masaki T, Suzuki R, Saeed M, Mori K, Matsuda M, Aizaki H, Ishii K, Maki N, Miyamura T, Matsuura Y, Wakita T, Suzuki T. 2010. Production of infectious hepatitis C virus by using RNA polymerase I-mediated transcription. J. Virol. 84:5824–5835. http://dx.doi.org/10.1128/JVI.02397-09.
47. Masaki T, Matsuura T, Ohkawa K, Miyamura T, Okazaki I, Watanabe T, Suzuki T. 2006. All-trans retinoic acid down-regulates human albumin gene expression through the induction of C/EBPβ-LIP. Biochem. J. 397:345–353. http://dx.doi.org/10.1042/BJ20051863.
48. Iwahori T, Matsuura T, Maehashi H, Sugo K, Saito M, Hosokawa M, Chiba K, Masaki T, Aizaki H, Ohkawa K, Suzuki T. 2003. CYP3A4 inducible model for in vitro analysis of human drug metabolism using a bioartificial liver. Hepatology 37:665–673. http://dx.doi.org/10.1053/jhep.2003.50094.
49. Li Q, Lau A, Morris TJ, Guo L, Fordyce CB, Stanley EF. 2004. A syntaxin 1, Gα(o), and N-type calcium channel complex at a presynaptic nerve terminal: analysis by quantitative immunocolocalization. J. Neurosci. 24:4070–4081. http://dx.doi.org/10.1523/JNEUROSCI.0346-04.2004.
50. Kim J, Lee D, Choe J. 1999. Hepatitis C virus NS5A protein is phosphorylated by casein kinase II. Biochem. Biophys. Res. Commun. 257:777–781. http://dx.doi.org/10.1006/bbrc.1999.0460.
51. Ide Y, Tanimoto A, Sasaguri Y, Padmanabhan R. 1997. Hepatitis C virus NS5A protein is phosphorylated in vitro by a stably bound protein kinase from HeLa cells and by cAMP-dependent protein kinase A-alpha catalytic subunit. Gene 201:151–158. http://dx.doi.org/10.1016/S0378-1119(97)00440-X.
52. Benga WJ, Krieger SE, Dimitrova M, Zeisel MB, Parnot M, Lupberger J, Hildt E, Luo G, McLauchlan J, Baumert TF, Schuster C. 2010. Apolipoprotein E interacts with hepatitis C virus nonstructural protein 5A and determines assembly of infectious particles. Hepatology 51:43–53. http://dx.doi.org/10.1002/hep.23278.
53. Farquhar MJ, Harris HJ, Diskar M, Jones S, Mee CJ, Nielsen SU, Brimacombe CL, Molina S, Toms GL, Maurel P, Howl J, Herberg FW, van Ijzendoorn SC, Balfe P, McKeating JA. 2008. Protein kinase A-dependent step(s) in hepatitis C virus entry and infectivity. J. Virol. 82:8797–8811. http://dx.doi.org/10.1128/JVI.00592-08.
54. Evans MJ, von Hahn T, Tscherne DM, Syder AJ, Panis M, Wolk B, Hatziioannou T, McKeating JA, Bieniasz PD, Rice CM. 2007. Claudin-1 is a hepatitis C virus co-receptor required for a late step in entry. Nature 446:801–805. http://dx.doi.org/10.1038/nature05654.
55. Matsumura T, Kato T, Sugiyama N, Tasaka-Fujita M, Murayama A, Masaki T, Wakita T, Imawari M. 2012. 25-Hydroxyvitamin D3 suppresses hepatitis C virus production. Hepatology 56:1231–1239. http://dx.doi.org/10.1002/hep.25763.
56. Miyanari Y, Atsuzawa K, Usuda N, Watashi K, Hishiki T, Zayas M, Bartenschlager R, Wakita T, Hijikata M, Shimotohno K. 2007. The lipid droplet is an important organelle for hepatitis C virus production. Nat. Cell Biol. 9:1089–1097. http://dx.doi.org/10.1038/ncb1631.
57. Ubersax JA, Ferrell JE, Jr. 2007. Mechanisms of specificity in protein phosphorylation. Nat. Rev. Mol. Cell Biol. 8:530–541. http://dx.doi.org/10.1038/nrm2203.
58. Ross-Thriepland D, Harris M. 2014. Insights into the complexity and functionality of hepatitis C virus NS5A phosphorylation. J. Virol. 88:1421–1432. http://dx.doi.org/10.1128/JVI.03017-13.
59. Fridell RA, Valera L, Qiu D, Kirk MJ, Wang C, Gao M. 2013. Intragenic complementation of hepatitis C virus NS5A RNA replication-defective alleles. J. Virol. 87:2320–2329. http://dx.doi.org/10.1128/JVI.02861-12.
60. Fridell RA, Qiu D, Valera L, Wang C, Rose RE, Gao M. 2011. Distinct functions of NS5A in hepatitis C virus RNA replication uncovered by studies with the NS5A inhibitor BMS-790052. J. Virol. 85:7312–7320. http://dx.doi.org/10.1128/JVI.00253-11.
61. Kim S, Welsch C, Yi M, Lemon SM. 2011. Regulation of the production of infectious genotype 1a hepatitis C virus by NS5A domain III. J. Virol. 85:6645–6656. http://dx.doi.org/10.1128/JVI.02156-10.
62. Qiu D, Lemm JA, O'Boyle DR, II, Sun JH, Nower PT, Nguyen V, Hamann LG, Snyder LB, Deon DH, Ruediger E, Meanwell NA, Belema M, Gao M, Fridell RA. 2011. The effects of NS5A inhibitors on NS5A phosphorylation, polyprotein processing and localization. J. Gen. Virol. 92:2502–2511. http://dx.doi.org/10.1099/vir.0.034801-0.
63. Camus G, Herker E, Modi AA, Haas JT, Ramage HR, Farese RV, Jr, Ott M. 2013. Diacylglycerol acyltransferase-1 localizes hepatitis C virus NS5A protein to lipid droplets and enhances NS5A interaction with the viral capsid core. J. Biol. Chem. 288:9915–9923. http://dx.doi.org/10.1074/jbc.M112.434910.
64. Gao L, Aizaki H, He JW, Lai MM. 2004. Interactions between viral nonstructural proteins and host protein hVAP-33 mediate the formation of hepatitis C virus RNA replication complex on lipid raft. J. Virol. 78:3480–3488. http://dx.doi.org/10.1128/JVI.78.7.3480-3488.2004.
65. Berger KL, Cooper JD, Heaton NS, Yoon R, Oakland TE, Jordan TX, Mateu G, Grakoui A, Randall G. 2009. Roles for endocytic trafficking and phosphatidylinositol 4-kinase III alpha in hepatitis C virus replication. Proc. Natl. Acad. Sci. U. S. A. 106:7577–7582. http://dx.doi.org/10.1073/pnas.0902693106.
66. Vaillancourt FH, Pilote L, Cartier M, Lippens J, Liuzzi M, Bethell RC, Cordingley MG, Kukolj G. 2009. Identification of a lipid kinase as a host factor involved in hepatitis C virus RNA replication. Virology 387:5–10. http://dx.doi.org/10.1016/j.virol.2009.02.039.
67. Borawski J, Troke P, Puyang X, Gibaja V, Zhao S, Mickanin C, Leighton-Davies J, Wilson CJ, Myer V, Cornellataracido I, Baryza J, Tallarico J, Joberty G, Bantscheff M, Schirle M, Bouwmeester T, Mathy JE, Lin K, Compton T, Labow M, Wiedmann B, Gaither LA. 2009. Class III phosphatidylinositol 4-kinase alpha and beta are novel host factor regulators of hepatitis C virus replication. J. Virol. 83:10058–10074. http://dx.doi.org/10.1128/JVI.02418-08.
68. Tai AW, Benita Y, Peng LF, Kim SS, Sakamoto N, Xavier RJ, Chung RT. 2009. A functional genomic screen identifies cellular cofactors of hepatitis C virus replication. Cell Host. Microbe 5:298–307. http://dx.doi.org/10.1016/j.chom.2009.02.001.
69. Li Q, Brass AL, Ng A, Hu Z, Xavier RJ, Liang TJ, Elledge SJ. 2009. A genome-wide genetic screen for host factors required for hepatitis C virus propagation. Proc. Natl. Acad. Sci. U. S. A. 106:16410–16415. http://dx.doi.org/10.1073/pnas.0907439106.
70. Trotard M, Lepere-Douard C, Regeard M, Piquet-Pellorce C, Lavillette D, Cosset FL, Gripon P, Le Seyec J. 2009. Kinases required in hepatitis C virus entry and replication highlighted by small interference RNA screening. FASEB J. 23:3780–3789. http://dx.doi.org/10.1096/fj.09-131920.
71. Reiss S, Rebhan I, Backes P, Romero-Brey I, Erfle H, Matula P, Kaderali L, Poenisch M, Blankenburg H, Hiet MS, Longerich T, Diehl S, Ramirez F, Balla T, Rohr K, Kaul A, Buhler S, Pepperkok R, Lengauer T, Albrecht M, Eils R, Schirmacher P, Lohmann V, Bartenschlager R. 2011. Recruitment and activation of a lipid kinase by hepatitis C virus NS5A is essential for integrity of the membranous replication compartment. Cell Host Microbe 9:32–45. http://dx.doi.org/10.1016/j.chom.2010.12.002.
72. Berger KL, Kelly SM, Jordan TX, Tartell MA, Randall G. 2011. Hepatitis C virus stimulates the phosphatidylinositol 4-kinase III alpha-dependent phosphatidylinositol 4-phosphate production that is essential for its replication. J. Virol. 85:8870–8883. http://dx.doi.org/10.1128/JVI.00059-11.
73. Reiss S, Harak C, Romero-Brey I, Radujkovic D, Klein R, Ruggieri A, Rebhan I, Bartenschlager R, Lohmann V. 2013. The lipid kinase phosphatidylinositol-4 kinase III alpha regulates the phosphorylation status of hepatitis C virus NS5A. PLoS Pathog. 9:e1003359. http://dx.doi.org/10.1371/journal.ppat.1003359.
74. Pietschmann T, Zayas M, Meuleman P, Long G, Appel N, Koutsoudakis G, Kallis S, Leroux-Roels G, Lohmann V, Bartenschlager R. 2009. Production of infectious genotype 1b virus particles in cell culture and impairment by replication enhancing mutations. PLoS Pathog. 5:e1000475. http://dx.doi.org/10.1371/journal.ppat.1000475.

## Supplemental Table S1. List of 404 Kinases Analyzed by AlphaScreen

| # | Kinases | Value | # | Kinases | Value | # | Kinases | Value | # | Kinases | Value |
|---|---|---|---|---|---|---|---|---|---|---|---|
| 1 | PIM1 | 24020 | 36 | MLKL | 2880 | 71 | DCAMKL1 | 1674 | 106 | CDKL2 | 1184 |
| 2 | LYN | 22342 | 37 | CK1g2 | 2602 | 72 | MAPKAPK2 | 1668 | 107 | CDK5 | 1180 |
| 3 | ULK4 | 21784 | 38 | CDKL3 | 2584 | 73 | JAK3 | 1664 | 108 | YANK2 | 1172 |
| 4 | Fused | 18910 | 39 | CK1g1 | 2560 | 74 | PAK1 | 1652 | 109 | STLK6 | 1162 |
| 5 | TGFbR1 | 15634 | 40 | SgK495 | 2558 | 75 | CK1d | 1608 | 110 | AMPKa2 | 1148 |
| 6 | MLK1 | 12242 | 41 | CK2a1 | 2534 | 76 | FGR | 1602 | 111 | MNK2 | 1144 |
| 7 | smMLCK | 10084 | 42 | PRPK | 2528 | 77 | CaMKK2 | 1578 | 112 | TYRO3 | 1140 |
| 8 | PDHK2 | 8868 | 43 | GSK3B | 2410 | 78 | SYK | 1576 | 113 | RIOK2 | 1116 |
| 9 | TSSK2 | 8310 | 44 | PITSLRE | 2304 | 79 | LOK | 1554 | 114 | MST3 | 1114 |
| 10 | HCK | 8250 | 45 | ULK3 | 2262 | 80 | SgK223 | 1548 | 115 | PKD2 | 1080 |
| 11 | PIM2 | 7340 | 46 | MAP2K2 | 2254 | 81 | TSSK4 | 1546 | 116 | MASTL | 1066 |
| 12 | DYRK3 | 5116 | 47 | CK1g3 | 2218 | 82 | SGK2 | 1530 | 117 | MYO3A | 1058 |
| 13 | CK2a2 | 5068 | 48 | ULK2 | 2212 | 83 | SRPK1 | 1526 | 118 | CASK | 1056 |
| 14 | JNK1 | 5048 | 49 | MAP2K6 | 2112 | 84 | RSK2 | 1496 | 119 | RIPK1 | 1054 |
| 15 | NEK7 | 5006 | 50 | OSR1 | 2108 | 85 | MNK1 | 1458 | 120 | LATS2 | 1044 |
| 16 | FGFR2 | 4930 | 51 | NRBP1 | 2076 | 86 | BMPR1A | 1444 | 121 | ILK | 1040 |
| 17 | TLK2 | 4716 | 52 | LIMK2 | 2036 | 87 | PINK1 | 1440 | 122 | TIF1a | 1038 |
| 18 | Wee1B | 4606 | 53 | CHED | 2018 | 88 | Slob | 1418 | 123 | PKCa | 1032 |
| 19 | RSKL2 | 4552 | 54 | CK1e | 2012 | 89 | SGK3 | 1400 | 124 | DAPK1 | 1026 |
| 20 | ROCK1 | 4502 | 55 | RNAseL | 1934 | 90 | MAP2K1 | 1386 | 125 | HIPK2 | 1022 |
| 21 | HUNK | 4448 | 56 | FRAP | 1932 | 91 | FAK | 1364 | 126 | JAK1 | 1014 |
| 22 | PKG2 | 4206 | 57 | FER | 1862 | 92 | MAP3K2 | 1358 | 127 | CaMK2g | 992 |
| 23 | FES | 3900 | 58 | PKACb | 1854 | 93 | CK1a | 1354 | 128 | JNK2 | 972 |
| 24 | SGK | 3782 | 59 | DDR1 | 1846 | 94 | ADCK1 | 1344 | 129 | TIE1 | 966 |
| 25 | HIPK1 | 3638 | 60 | CaMK2b | 1828 | 95 | CDK8 | 1302 | 130 | PKD3 | 954 |
| 26 | MELK | 3600 | 61 | p70S6K | 1824 | 96 | ZC1/HGK | 1262 | 131 | Erk2 | 932 |
| 27 | MARK3 | 3414 | 62 | CaMK1a | 1772 | 97 | NIM1 | 1252 | 132 | NIK | 924 |
| 28 | RET | 3380 | 63 | RSK1 | 1758 | 98 | PHKg1 | 1248 | 133 | NEK11 | 920 |
| 29 | ADCK3 | 3380 | 64 | Erk3 | 1744 | 99 | PDGFRb | 1244 | 134 | Trb1 | 916 |
| 30 | VRK1 | 3348 | 65 | SCYL2 | 1740 | 100 | ALK2 | 1238 | 135 | MAP3K4 | 914 |
| 31 | TAK1 | 3304 | 66 | RIPK2 | 1692 | 101 | MYT1 | 1236 | 136 | KHS2 | 914 |
| 32 | PLK1 | 3230 | 67 | BUB1 | 1692 | 102 | PKCd | 1218 | 137 | PDGFRa | 912 |
| 33 | PKN2 | 3152 | 68 | p38a | 1684 | 103 | CLIK1 | 1218 | 138 | NEK6 | 904 |
| 34 | KIS | 3126 | 69 | skMLCK | 1678 | 104 | Trad | 1204 | 139 | FLT1 | 902 |
| 35 | AurB | 3102 | 70 | ARAF | 1676 | 105 | AKT2 | 1198 | 140 | AKT1 | 898 |

## Supplemental Table S1. List of 404 Kinases Analyzed by AlphaScreen

| # | Kinases | Value | # | Kinases | Value | # | Kinases | Value | # | Kinases | Value |
|---|---|---|---|---|---|---|---|---|---|---|---|
| 141 | BRD2 | 886 | 176 | TESK1 | 740 | 211 | SPEG | 610 | 246 | SRPK2 | 532 |
| 142 | MOK | 874 | 177 | CSK | 740 | 212 | CaMK2d | 610 | 247 | PKCh | 530 |
| 143 | ROR2 | 870 | 178 | SgK288 | 726 | 213 | YES | 608 | 248 | IRR | 530 |
| 144 | GCN2 | 864 | 179 | FLT3 | 710 | 214 | PCTAIRE2 | 606 | 249 | IRAK2 | 530 |
| 145 | SCYL3 | 858 | 180 | CDK3 | 710 | 215 | LCK | 600 | 250 | TXK | 528 |
| 146 | CDKL1 | 854 | 181 | IKKe | 706 | 216 | EphA7 | 598 | 251 | AlphaK3 | 526 |
| 147 | SRC | 840 | 182 | CDK4 | 706 | 217 | CDK2 | 598 | 252 | BARK2 | 516 |
| 148 | DYRK1B | 836 | 183 | PDHK3 | 704 | 218 | GPRK4 | 596 | 253 | JAK2 | 510 |
| 149 | CaMK1g | 834 | 184 | PIK3R4 | 702 | 219 | PKCb | 594 | 254 | p38b | 508 |
| 150 | PAK2 | 822 | 185 | TRKB | 700 | 220 | BLK | 594 | 255 | FYN | 508 |
| 151 | PKR | 812 | 186 | CDK10 | 700 | 221 | STLK5 | 590 | 256 | NEK1 | 506 |
| 152 | PDHK4 | 812 | 187 | IRAK3 | 696 | 222 | TIF1b | 584 | 257 | NDR1 | 506 |
| 153 | caMLCK | 812 | 188 | CLK4 | 694 | 223 | LRRK2 | 584 | 258 | PHKg2 | 500 |
| 154 | IRAK1 | 806 | 189 | MAK | 690 | 224 | DAPK3 | 584 | 259 | CLK2 | 500 |
| 155 | CTK | 806 | 190 | BMPR1B | 690 | 225 | VRK3 | 582 | 260 | DDR2 | 498 |
| 156 | JNK3 | 802 | 191 | MUSK | 688 | 226 | TSSK1 | 576 | 261 | TNK1 | 496 |
| 157 | RYK | 798 | 192 | KDR | 688 | 227 | CRIK | 576 | 262 | p70S6Kb | 496 |
| 158 | HER4/ErbB4 | 794 | 193 | PKCe | 678 | 228 | ULK1 | 572 | 263 | TAO3 | 494 |
| 159 | MST2 | 788 | 194 | BARK1 | 678 | 229 | TESK2 | 572 | 264 | MLK2 | 494 |
| 160 | MAP3K3 | 788 | 195 | SgK196 | 668 | 230 | PKN1 | 572 | 265 | NEK5 | 492 |
| 161 | DYRK1A | 784 | 196 | ACTR2 | 664 | 231 | PKCg | 570 | 266 | CCRK | 492 |
| 162 | eEF2K | 778 | 197 | PRKX | 658 | 232 | EphA3 | 570 | 267 | CaMKK1 | 490 |
| 163 | CHK1 | 774 | 198 | p38g | 658 | 233 | ALK4 | 564 | 268 | BMX | 484 |
| 164 | DAPK2 | 772 | 199 | MSK2 | 652 | 234 | A6r | 564 | 269 | PAK5 | 474 |
| 165 | RIPK3 | 770 | 200 | INSR | 652 | 235 | EphA1 | 562 | 270 | TTBK1 | 470 |
| 166 | DCAMKL3 | 766 | 201 | MAPKAPK5 | 644 | 236 | EphB4 | 558 | 271 | Trb3 | 470 |
| 167 | SgK269 | 762 | 202 | TBCK | 642 | 237 | ZAP70 | 556 | 272 | G11 | 466 |
| 168 | CDKL5 | 762 | 203 | HER3/ErbB3 | 640 | 238 | H11 | 552 | 273 | IKKb | 464 |
| 169 | TYK2 | 760 | 204 | TTK | 638 | 239 | GPRK5 | 548 | 274 | CaMK2a | 464 |
| 170 | NuaK2 | 760 | 205 | TAO2 | 638 | 240 | COT | 546 | 275 | Trb2 | 462 |
| 171 | IKKa | 758 | 206 | STK33 | 628 | 241 | NDR2 | 542 | 276 | EphA4 | 462 |
| 172 | RSK4 | 756 | 207 | SNRK | 622 | 242 | DRAK1 | 542 | 277 | DYRK2 | 460 |
| 173 | DNAPK | 750 | 208 | MST1 | 620 | 243 | HRI | 538 | 278 | TRKA | 458 |
| 174 | YSK1 | 748 | 209 | TRKC | 614 | 244 | MAPKAPK3 | 536 | 279 | FGFR1 | 458 |
| 175 | RSK3 | 742 | 210 | FRK | 612 | 245 | AurC | 534 | 280 | MAP3K6 | 456 |

## Supplemental Table S1. List of 404 Kinases Analyzed by AlphaScreen

| # | Kinases | Value | # | Kinases | Value | # | Kinases | Value | # | Kinases | Value |
|---|---|---|---|---|---|---|---|---|---|---|---|
| 281 | SgK496 | 454 | 312 | ANKRD3 | 396 | 343 | PIM3 | 352 | 374 | DCAMKL2 | 284 |
| 282 | KSR1 | 454 | 313 | BCKDK | 394 | 344 | ITK | 352 | 375 | GCK | 282 |
| 283 | CLK1 | 454 | 314 | CDK6 | 392 | 345 | CDK11 | 350 | 376 | PRP4 | 280 |
| 284 | IRE2 | 452 | 315 | ADCK4 | 390 | 346 | CDC2 | 348 | 377 | MLK4 | 274 |
| 285 | TSSK3 | 446 | 316 | TBK1 | 388 | 347 | ABL | 346 | 378 | GPRK6 | 274 |
| 286 | CYGD | 438 | 317 | CaMK1b | 388 | 348 | PAK6 | 344 | 379 | DLK | 272 |
| 287 | PKCt | 436 | 318 | SuRTK106 | 386 | 349 | MARK1 | 344 | 380 | PSKH1 | 270 |
| 288 | PCTAIRE3 | 432 | 319 | PKG1 | 386 | 350 | FGFR3 | 342 | 381 | NEK2 | 268 |
| 289 | AlphaK1 | 432 | 320 | PFTAIRE1 | 386 | 351 | BUBR1 | 342 | 382 | AXL | 268 |
| 290 | EphB1 | 430 | 321 | NEK8 | 386 | 352 | p38d | 340 | 383 | CDK9 | 266 |
| 291 | MET | 428 | 322 | ROR1 | 382 | 353 | MST4 | 338 | 384 | Erk4 | 264 |
| 292 | IRE1 | 428 | 323 | LMR1 | 382 | 354 | CaMK4 | 336 | 385 | PYK2 | 262 |
| 293 | MARK2 | 424 | 324 | GAK | 382 | 355 | AMPKa1 | 334 | 386 | ALK7 | 260 |
| 294 | CCK4 | 424 | 325 | SCYL1 | 380 | 356 | NEK4 | 332 | 387 | PDK1 | 256 |
| 295 | ZAK | 422 | 326 | MAP3K7 | 378 | 357 | BRK | 332 | 388 | PASK | 256 |
| 296 | HER2/ErbB2 | 420 | 327 | IGF1R | 372 | 358 | EphA6 | 330 | 389 | EphA2 | 256 |
| 297 | EphB6 | 420 | 328 | AurA | 370 | 359 | TIE2 | 324 | 390 | MAST2 | 254 |
| 298 | BIKE | 420 | 329 | SSTK | 368 | 360 | PAK3 | 324 | 391 | MPSK1 | 252 |
| 299 | FASTK | 418 | 330 | RSKL1 | 368 | 361 | MARK4 | 324 | 392 | CDK7 | 252 |
| 300 | BRD3 | 416 | 331 | GSK3A | 366 | 362 | PCTAIRE1 | 320 | 393 | SIK | 250 |
| 301 | LIMK1 | 414 | 332 | MAP2K5 | 364 | 363 | MAP2K3 | 320 | 394 | DRAK2 | 250 |
| 302 | HIPK3 | 414 | 333 | FMS | 364 | 364 | EphA5 | 320 | 395 | YANK3 | 244 |
| 303 | VRK2 | 408 | 334 | MAST4 | 362 | 365 | PKCz | 318 | 396 | PAK4 | 244 |
| 304 | HSER | 408 | 335 | FGFR4 | 362 | 366 | TEC | 312 | 397 | KHS1 | 244 |
| 305 | QIK | 406 | 336 | EphB3 | 360 | 367 | A6 | 310 | 398 | ZC2/TNIK | 240 |
| 306 | CaMK1d | 406 | 337 | TLK1 | 358 | 368 | RIOK3 | 304 | 399 | RIOK1 | 240 |
| 307 | RON | 404 | 338 | CHK2 | 358 | 369 | STLK3 | 298 | 400 | MAP2K7 | 240 |
| 308 | FLT4 | 402 | 339 | ACTR2B | 358 | 370 | Erk5 | 296 | 401 | PFTAIRE2 | 236 |
| 309 | CLK3 | 402 | 340 | PEK | 356 | 371 | PKCi | 290 | 402 | MYO3B | 224 |
| 310 | RAF1 | 400 | 341 | PDHK1 | 356 | 372 | PBK | 284 | 403 | MAP2K4 | 218 |
| 311 | ICK | 398 | 342 | TGFbR2 | 352 | 373 | IRAK4 | 284 | 404 | KIT | 216 |

**Footnotes.**

- Kinases are sorted in descending order (largest value first) according to AlphaScreen values.
- Data shown are mean values of duplicate experiments.

**Supplemental Table S2.**
**Serine/Threonine Kinases Analyzed by *In Vitro* Phosphorylation Assay**

| | | Relative Kinase Activity | | | | Relative Kinase Activity | |
|---|---|---|---|---|---|---|---|
| Kinases | LU | FL | D3 | Kinases | LU | FL | D3 |
| PIM1 | 24020 | 1.77 | 4.06 | CKI-γ1 | 2560 | n/a* | 138.69 |
| ULK4 | 21784 | 1.02 | 0.79 | PRPK | 2528 | 1.57 | 3.04 |
| Fused | 18910 | 0.84 | 0.92 | GSK3B | 2410 | 1.53 | 1.58 |
| TGFβR1 | 15634 | 1.10 | 2.12 | PITSLRE | 2304 | 2.26 | 2.94 |
| MLK1 | 12242 | 2.69 | 0.64 | CKI-γ3 | 2218 | 0.23 | 52.51 |
| smMLCK | 10084 | 1.41 | 0.92 | MAP2K6 | 2112 | n/a | 0.14 |
| PDHK2 | 8868 | 0.91 | 2.54 | NRBP1 | 2076 | n/a | 0.97 |
| TSSK2 | 8310 | 4.24 | 14.94 | LIMK2 | 2036 | 0.80 | 0.47 |
| PIM2 | 7340 | 0.95 | 1.00 | CHED | 2018 | n/a | 1.50 |
| DYRK3 | 5116 | 1.62 | 0.99 | CKI-ε | 2012 | 7.95 | 9.48 |
| CKII-α' | 5068 | 2.30 | 8.20 | RNAseL | 1934 | n/a | 1.15 |
| JNK1 | 5048 | 0.64 | 1.95 | FRAP | 1932 | n/a | 1.30 |
| NEK7 | 5006 | 1.69 | 1.52 | PKACβ | 1854 | 0.15 | 69.54 |
| TLK2 | 4716 | 1.27 | 0.96 | CaMK2β | 1828 | 1.53 | 0.97 |
| Wee1B | 4606 | 1.27 | 2.62 | RSK1 | 1758 | 0.78 | 0.55 |
| RSKL2 | 4552 | n/a | 1.27 | Erk3 | 1744 | n/a | 1.63 |
| ROCK1 | 4502 | n/a* | 1.26 | BUB1 | 1692 | 1.02 | 0.95 |
| HUNK | 4448 | 1.67 | 1.00 | p38α | 1684 | n/a | 1.01 |
| PKG2 | 4206 | 0.22 | 2.44 | skMLCK | 1678 | n/a | 1.45 |
| SGK | 3782 | 2.28 | 1.19 | DCAMKL1 | 1674 | n/a | 5.55 |
| MARK3 | 3414 | n/a | 4.48 | MAPKAPK2 | 1668 | 1.39 | 1.63 |
| ADCK3 | 3380 | n/a | 1.49 | CaMKK2 | 1578 | n/a | 3.49 |
| VRK1 | 3348 | 2.41 | 1.75 | SGK2 | 1530 | n/a | 1.26 |
| Plk1 | 3230 | 2.70 | 44.65 | MNK1 | 1458 | 1.69 | 2.84 |
| PKN2 | 3152 | 0.80 | 1.99 | Slob | 1418 | n/a | 0.63 |
| KIS | 3126 | 3.36 | 1.11 | MAP3K2 | 1358 | n/a | 1.22 |
| CKI-γ2 | 2602 | 4.31 | 3.15 | CKI-α | 1354 | 4.66 | 1.00 |
| CDKL3 | 2584 | 0.98 | 3.09 | | | | |

**Footnotes.** LU: light unit in AlphaScreen; FL: full-length NS5A; D3: domain III of NS5A; n/a: not assessed due to low amounts of full-length NS5A; n/a*: not assessed due to overlap between purified kinases and NS5A on the gel; Relative Kinase Activity: fold increase of the *in vitro* kinase activity of each kinase relative to that of DHFR.

**Supplemental Table S3. NS5A Peptides Identified by LC-MS/MS**

| m/z | Mass | Charge State | Peptide Score | Peptide Sequence | Location in NS5A (aa) | | | Modification (Residue) | Knockdown | No. of Peptide |
|---|---|---|---|---|---|---|---|---|---|---|
| 1196.5 | 3586.6 | 3 | 25.1 | ATCTTHSNTYDVDMVDANLLMEGGVAQTEPESR | 241 | - | 273 | Oxidation (M) | Ctrl | 1 |
| 1182.6 | 2363.2 | 2 | 31.5 | LARGSPPSEASSSVSQLSAPSLR | 218 | - | 240 | Phosphorylation (S/T) | Ctrl | 1 |
| 1182.6 | 2363.2 | 2 | 27.6 | LARGSPPSEASSSVSQLSAPSLR | 218 | - | 240 | Phosphorylation (S/T) | CKI-α | 1 |
| 1119.6 | 2237.1 | 2 | 27.3 | ALPAWARPDYNPPLVESWR | 308 | - | 326 | | Ctrl | 1 |
| 1072.6 | 2143.2 | 2 | 63.4 | RTVGLSESTISEALQQLAIK | 355 | - | 374 | | Ctrl | 5 |
| 1072.6 | 2143.2 | 2 | 99.2 | RTVGLSESTISEALQQLAIK | 355 | - | 374 | | CKI-α | 3 |
| 1052.5 | 2102.9 | 2 | 25.0 | GSPPSEASSSVSQLSAPSLR | 221 | - | 240 | Phosphorylation (S/T) | Ctrl | 1 |
| 1034.5 | 2067.0 | 2 | 34.0 | TVGLSESTISEALQQLAIK | 356 | - | 374 | Phosphorylation (S/T) | Ctrl | 1 |
| 1012.5 | 2022.9 | 2 | 99.4 | GSPPSEASSSVSQLSAPSLR | 221 | - | 240 | Phosphorylation (S/T) | Ctrl | 8 |
| 1012.5 | 2022.9 | 2 | 96.2 | GSPPSEASSSVSQLSAPSLR | 221 | - | 240 | Phosphorylation (S/T) | CKI-α | 13 |
| 1012.5 | 2022.9 | 2 | 72.5 | GSPPSEASSSVSQLSAPSLR | 221 | - | 240 | Phosphorylation (S/T) | Ctrl | 2 |
| 1012.5 | 2022.9 | 2 | 70.8 | GSPPSEASSSVSQLSAPSLR | 221 | - | 240 | Phosphorylation (S/T) | CKI-α | 2 |
| 994.5 | 1987.1 | 2 | 123.0 | TVGLSESTISEALQQLAIK | 356 | - | 374 | | Ctrl | 10 |
| 994.5 | 1987.1 | 2 | 107.0 | TVGLSESTISEALQQLAIK | 356 | - | 374 | | CKI-α | 10 |
| 989.5 | 1977.0 | 2 | 65.0 | RPDYQPPTVAGCALPPPK | 327 | - | 344 | Propionamide (C) | CKI-α | 8 |
| 972.5 | 1943.0 | 2 | 122.3 | GSPPSEASSSVSQLSAPSLR | 221 | - | 240 | | Ctrl | 48 |
| 972.5 | 1943.0 | 2 | 132.3 | GSPPSEASSSVSQLSAPSLR | 221 | - | 240 | | CKI-α | 73 |
| 968.8 | 2903.4 | 3 | 60.7 | VAASEYAEVTQHGSYSYVTGLTTDNLK | 113 | - | 139 | | Ctrl | 5 |
| 968.8 | 2903.4 | 3 | 70.2 | VAASEYAEVTQHGSYSYVTGLTTDNLK | 113 | - | 139 | | CKI-α | 12 |
| 954.0 | 1906.0 | 2 | 59.0 | RPDYQPPTVAGCALPPPK | 327 | - | 344 | | CKI-α | 8 |
| 863.9 | 1725.8 | 2 | 81.8 | SMLTDPPHITAETAAR | 201 | - | 216 | Oxidation (M) | Ctrl | 20 |
| 863.9 | 1725.8 | 2 | 87.0 | SMLTDPPHITAETAAR | 201 | - | 216 | Oxidation (M) | CKI-α | 75 |
| 855.9 | 1709.8 | 2 | 86.6 | SMLTDPPHITAETAAR | 201 | - | 216 | | Ctrl | 23 |
| 855.9 | 1709.8 | 2 | 86.4 | SMLTDPPHITAETAAR | 201 | - | 216 | | CKI-α | 17 |
| 842.8 | 2525.3 | 3 | 58.5 | IPCQLPSPEFFSWVDGVQIHR | 140 | - | 160 | Propionamide (C) | Ctrl | 2 |
| 842.8 | 2525.3 | 3 | 53.9 | IPCQLPSPEFFSWVDGVQIHR | 140 | - | 160 | Propionamide (C) | CKI-α | 1 |
| 819.1 | 2454.2 | 3 | 68.6 | IPCQLPSPEFFSWVDGVQIHR | 140 | - | 160 | | Ctrl | 2 |
| 819.1 | 2454.2 | 3 | 53.2 | IPCQLPSPEFFSWVDGVQIHR | 140 | - | 160 | | CKI-α | 1 |
| 799.4 | 1596.8 | 2 | 60.8 | GYKGVWAGTGIMTTR | 42 | - | 56 | | Ctrl | 2 |
| 799.4 | 1596.8 | 2 | 72.0 | GYKGVWAGTGIMTTR | 42 | - | 56 | | CKI-α | 2 |
| 794.1 | 2379.3 | 3 | 59.0 | RRTVGLSESTISEALQQLAIK | 354 | - | 374 | Phosphorylation (S/T) | CKI-α | 1 |
| 788.7 | 2363.1 | 3 | 46.0 | LARGSPPSEASSSVSQLSAPSLR | 218 | - | 240 | Phosphorylation (S/T) | Ctrl | 3 |
| 788.7 | 2363.1 | 3 | 54.4 | LARGSPPSEASSSVSQLSAPSLR | 218 | - | 240 | Phosphorylation (S/T) | CKI-α | 2 |
| 679.0 | 2034.1 | 3 | 75.4 | RPDYQPPTVAGCALPPPKK | 327 | - | 345 | | Ctrl | 6 |
| 679.0 | 2034.1 | 3 | 83.9 | RPDYQPPTVAGCALPPPKK | 327 | - | 345 | | CKI-α | 4 |
| 675.3 | 2022.9 | 3 | 36.9 | GSPPSEASSSVSQLSAPSLR | 221 | - | 240 | Phosphorylation (S/T) | Ctrl | 1 |
| 675.3 | 2022.9 | 3 | 25.0 | GSPPSEASSSVSQLSAPSLR | 221 | - | 240 | Phosphorylation (S/T) | Ctrl | 1 |
| 666.8 | 1331.6 | 2 | 67.7 | CPCGANISGNVR | 57 | - | 68 | Propionamide (C) | Ctrl | 2 |
| 666.8 | 1331.6 | 2 | 64.1 | CPCGANISGNVR | 57 | - | 68 | Propionamide (C) | CKI-α | 2 |
| 660.0 | 1977.0 | 3 | 74.2 | RPDYQPPTVAGCALPPPK | 327 | - | 344 | Propionamide (C) | Ctrl | 8 |
| 637.4 | 1272.7 | 2 | 44.4 | LPGLPFISCQK | 31 | - | 41 | Propionamide (C) | Ctrl | 4 |
| 637.4 | 1272.7 | 2 | 53.0 | LPGLPFISCQK | 31 | - | 41 | Propionamide (C) | CKI-α | 4 |
| 636.3 | 1906.0 | 3 | 68.9 | RPDYQPPTVAGCALPPPK | 327 | - | 344 | | Ctrl | 13 |
| 633.3 | 1264.6 | 2 | 66.6 | GVWAGTGIMTTR | 45 | - | 56 | Oxidation (M) | Ctrl | 6 |
| 633.3 | 1264.6 | 2 | 64.4 | GVWAGTGIMTTR | 45 | - | 56 | Oxidation (M) | CKI-α | 8 |
| 631.3 | 1260.6 | 2 | 74.9 | CPCGANISGNVR | 57 | - | 68 | Propionamide (C) | Ctrl | 1 |
| 631.3 | 1260.6 | 2 | 55.5 | CPCGANISGNVR | 57 | - | 68 | Propionamide (C) | CKI-α | 1 |
| 631.3 | 1260.6 | 2 | 72.7 | CPCGANISGNVR | 57 | - | 68 | Propionamide (C) | Ctrl | 2 |
| 631.3 | 1260.6 | 2 | 61.2 | CPCGANISGNVR | 57 | - | 68 | Propionamide (C) | CKI-α | 2 |
| 625.3 | 1248.6 | 2 | 75.5 | GVWAGTGIMTTR | 45 | - | 56 | | Ctrl | 71 |
| 625.3 | 1248.6 | 2 | 69.6 | GVWAGTGIMTTR | 45 | - | 56 | | CKI-α | 42 |
| 604.3 | 1206.7 | 2 | 27.3 | FAPTPKPFFR | 161 | - | 170 | | CKI-α | 2 |
| 601.8 | 1201.7 | 2 | 45.3 | LPGLPFISCQK | 31 | - | 41 | | Ctrl | 6 |
| 601.8 | 1201.7 | 2 | 51.6 | LPGLPFISCQK | 31 | - | 41 | | CKI-α | 5 |
| 595.8 | 1189.5 | 2 | 79.8 | CPCGANISGNVR | 57 | - | 68 | | Ctrl | 9 |
| 595.8 | 1189.5 | 2 | 74.6 | CPCGANISGNVR | 57 | - | 68 | | CKI-α | 11 |
| 550.3 | 1098.6 | 2 | 39.7 | KAPTPPPRR | 345 | - | 353 | Phosphorylation (S/T) | Ctrl | 10 |
| 550.3 | 1098.6 | 2 | 33.6 | KAPTPPPRR | 345 | - | 353 | Phosphorylation (S/T) | CKI-α | 8 |
| 510.3 | 1018.6 | 2 | 40.4 | KAPTPPPRR | 345 | - | 353 | | Ctrl | 9 |
| 510.3 | 1018.6 | 2 | 28.8 | KAPTPPPRR | 345 | - | 353 | | CKI-α | 4 |
| 472.2 | 942.5 | 2 | 45.1 | KAPTPPPR | 345 | - | 352 | Phosphorylation (S/T) | Ctrl | 6 |
| 472.2 | 942.5 | 2 | 30.7 | KAPTPPPR | 345 | - | 352 | Phosphorylation (S/T) | CKI-α | 6 |
| 446.3 | 890.5 | 2 | 31.4 | APTPPPRR | 346 | - | 353 | | CKI-α | 1 |
| 432.3 | 862.5 | 2 | 35.3 | KAPTPPPR | 345 | - | 352 | | Ctrl | 3 |
| 432.3 | 862.5 | 2 | 35.3 | KAPTPPPR | 345 | - | 352 | | CKI-α | 2 |
| 374.7 | 747.4 | 2 | 25.8 | NWLTSK | 21 | - | 26 | | CKI-α | 1 |
| 353.2 | 704.4 | 2 | 36.0 | SGSWLR | 1 | | 6 | | Ctrl | 2 |
| 353.2 | 704.4 | 2 | 43.0 | SGSWLR | 1 | - | 6 | | CKI-α | 2 |
| | | | | | | | | | Total | 629 |

**SUPPLEMENTAL TABLE S3. NS5A Peptides Identified by LC-MS/MS**

**Footnotes.** *m/z*: mass-to-charge ratio; Mass: molecular weight of a peptide; Charge State: number of charges of peptide ions; Peptide Score: parameter for peptide selection, and a minimum peptide score of 25 is used in this study; No. of Peptide: number of peptides identified. Peptides #1, #2, and #3 are highlighted in green, blue, and yellow, respectively. Phosphopeptides are indicated in bold red letters. Modified amino acids are underlined.

# Chapter 7
# Hepatic Differentiation of Human Embryonic Stem Cells and Induced Pluripotent Stem Cells by Two- and Three-Dimensional Culture Systems In Vitro

**Maiko Higuchi and Hiroyuki Mizuguchi**

**Abstract** Hepatocytes differentiated from human embryonic stem cells (hESCs) or induced pluripotent stem cells (hiPSCs) have a wide range of potential applications in biomedical research, drug discovery, and the treatment of liver disease. In this review, we provide an up-to-date overview of the wide variety of hepatic differentiation protocols. Moreover, we discuss the application of these protocols to three-dimensional culture systems in an attempt to induce hepatocyte-like cells with high hepatic functions.

**Keywords** Differentiation • ES cells • Hepatocytes • iPS cells • Three-dimensional culture

## 7.1 Hepatocytes in Cell-Based Therapy and Drug Discovery

The incidence of liver disease such as viral hepatitis, autoimmune hepatic disorders, fatty liver disease, and hepatic carcinoma is increasing worldwide [1]. Although the optimal treatment for end-stage liver disease is orthotopic liver transplantation, the

M. Higuchi
Laboratory of Biochemistry and Molecular Biology, Graduate School of Pharmaceutical Sciences, Osaka University, Osaka 565-0871, Japan

H. Mizuguchi (✉)
Laboratory of Biochemistry and Molecular Biology, Graduate School of Pharmaceutical Sciences, Osaka University, Osaka 565-0871, Japan

Laboratory of Hepatocyte Differentiation, National Institute of Biomedical Innovation, Osaka 567-0085, Japan

The Center for Advanced Medical Engineering and Informatics, Osaka University, Osaka 565-0871, Japan

iPS Cell-Based Research Project on Hepatic Toxicity and Metabolism, Graduate School of Pharmaceutical Sciences, Osaka University, Osaka 565-0871, Japan
e-mail: mizuguch@phs.osaka-u.ac.jp



M. Akashi et al. (eds.), *Engineered Cell Manipulation for Biomedical Application*, Nanomedicine and Nanotoxicology,
DOI 10.1007/978-4-431-55139-3_7

major limitation of such treatment is the shortage of donor livers. The liver is composed of several types of cells, including hepatocytes, endothelial cells, Kupffer cells, stellate cells, and hematopoietic cells. Of these cells, hepatocytes play the most important role in major liver functions. Hepatocytes have many functions, including carbohydrate metabolism, glycogen storage, lipid metabolism, urea synthesis, drug detoxification, production of plasma proteins, and destruction of erythrocytes [2]. Therefore, the transplantation of hepatocytes has been considered an effective treatment alternative to orthotopic liver transplantation [3]. However, such a treatment requires an unlimited source of hepatocytes. Hepatocytes are useful for not only regenerative medicine but biomedical research and drug discovery. They are particularly useful for drug screenings, such as for the determination of metabolic and toxicological properties of drug compounds in in vitro models. Primary human hepatocytes are the current standard in vitro model, but isolated hepatocytes lose their functions rapidly even under optimized culture conditions [4, 5]. The use of human hepatocytes is limited by the scarcity of primary tissue from healthy donors. Donor-to-donor and batch-to-batch variations are also significant problems. Moreover, human hepatocytes can no longer proliferate in in vitro culture [6]. These are crucial issues for various applications, and new and unlimited sources of human hepatocytes are urgently required to address them.

## 7.2 Hepatic Differentiation of hESCs/hiPSCs in Two-Dimensional Culture

hESCs and hiPSCs could be established as promising new resources for obtaining human hepatocytes. Abe et al. [7] and Levinson-Dushnik et al. [8] demonstrated that mouse ESCs (mESCs) were capable of differentiating into endodermal cells. Hamasaki et al. [9] reported that hepatocyte-like cells were induced from mESCs by using humoral factors. Rambhatla et al. demonstrated the differentiation of hESCs into hepatocyte-like cells for the first time [10]. Since then, many studies have been initiated to enhance the hepatic differentiation efficiency and the functional qualities of the hepatocyte-like cells [11–16].

Hepatic differentiation from hiPSCs has been achieved using similar protocols as for hESCs [17–20]. iPSCs were generated from somatic cells as a result of the overexpression of four reprogramming factors (Oct3/4, Sox2, Klf-4, and c-Myc) [21, 22]. Consequently, hiPSCs provide the opportunity to generate individual-specific hepatocyte-like cells. For example, drug metabolism capacity differs among individuals [23], and thus it is difficult to make a precise prediction of drug toxicity by using hepatocytes isolated from a single donor or hESC-derived hepatocytes. A hepatotoxicity screening utilizing hiPSC-derived hepatocyte-like cells would allow the investigation of individual drug metabolism capacity. Moreover, hiPSC-derived hepatocytes generated from patients suffering from a particular disease could provide a source for the disease study and disease modeling [24, 25]. These application would be expected to lead to the discovery of novel drugs.

### 7.2.1 *Stepwise Hepatic Differentiation from hESCs/hiPSCs*

The general strategy for hepatic differentiation from hESCs/hiPSCs is a stepwise culture with the addition of growth factors or cytokines [11, 20] (Fig. 7.1), which mimics the in vivo microenvironment during liver development [26, 27] (Fig. 7.2).

Gastrulation of the vertebrate embryo starts with the formation of three germ layers: the ectoderm, mesoderm, and endoderm. The endoderm differentiates into various organs, including the liver, pancreas, lungs, intestine, and stomach. To examine the molecular mechanisms of endoderm specification during early embryogenesis, endoderm differentiation from ESCs has been widely investigated as an in vitro model [28].

In definitive endoderm (DE) differentiation, it is well known that nodal signaling, which involves members of the transforming growth factor-β super family, plays a crucial role and induces the expression of endoderm-related genes [29]. Activin A, a member of the nodal family, is a ligand of the type II activin receptor and can transmit a downstream signal by using Smad adaptor proteins [30–32]. D'Amour et al. accomplished the differentiation of hESCs to DE by using activin A [32]. Recently, protocols using the combination of activin A with other factors such as fibroblast growth factor (FGF) 2 or Wint3a have been also applied to efficiently induce the DE [33, 34, 14].

Hepatic differentiation from the DE is divided into two steps: hepatic specification and hepatic maturation. In the hepatic specification step, the DE differentiates into hepatoblasts that express alpha-fetoprotein (AFP), transthyretin, and albumin (ALB) [35–37]. At this stage, the interaction of FGFs with bone morphogenetic

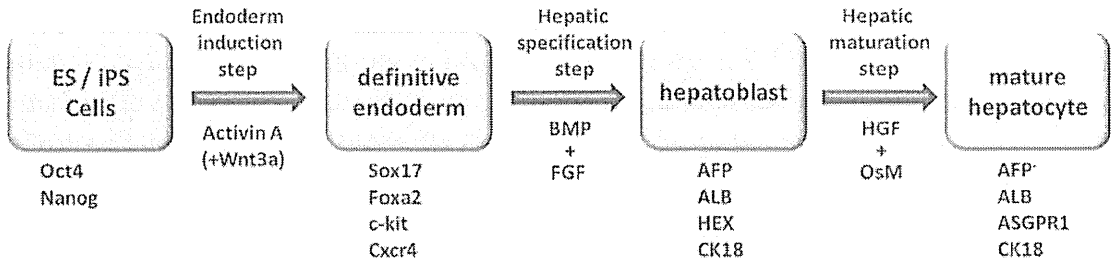


**Fig. 7.1** In vitro hepatic differentiation from hESCs/hiPSCs

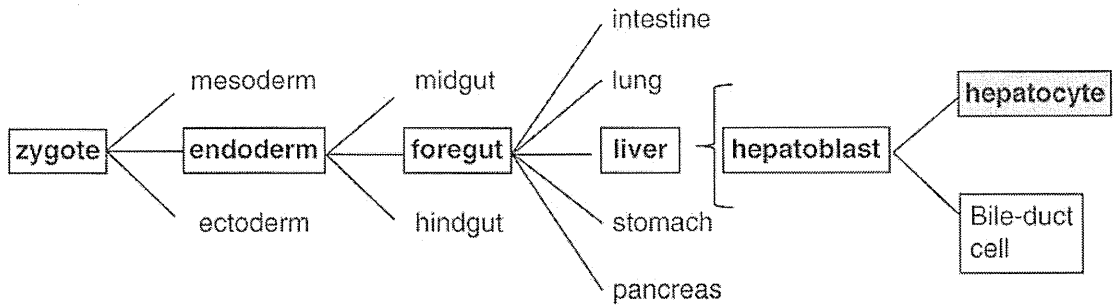


**Fig. 7.2** The cell lineage steps during hepatic development

protein (BMP) 2 or BMP4 is important for the induction of hepatocyte-related genes [27, 38]. The combination of FGF4 and BMP2 promotes hepatic specification from human ESC-derived DE cells [13]. Similar results were obtained by using the combinations of aFGF and BMP4, bFGF and BMP4, or FGF4 and BMP4 [13, 33].

It is known that hepatoblasts differentiate into two distinct lineages, hepatocytes and cholangiocytes. During the fetal hepatic maturation, growth factors that are secreted by surrounding non-parenchymal liver cells, such as hepatocyte growth factor (HGF) and oncostatin M (OsM), are essential for hepatic maturation [39]. HGF enhances hepatocyte proliferation but inhibits biliary differentiation by blocking notch signaling [40]. Although HGF is widely used for inducing hepatic phenotypes (e.g., ALB and dipeptidyl peptidase IV expression) [16, 41, 42], this is not enough to induce functional mature hepatocytes [42, 43]. OsM, which is expressed in hematopoietic cells in the fetal liver [43, 44], promotes the hepatic differentiation from hepatoblast cells [39, 40, 45]. Furthermore, supplementation of the culture medium with dexamethasone, a glucocorticoid hormone, induces the production of mature hepatocyte-specific proteins and also supports the maturation process of the hepatocytes together with OsM [14, 15, 18].

### *7.2.2 Hepatic Differentiation from hESCs/hiPSCs by Transduction of Hepatic Lineage-Specific Transcription Factors*

DE differentiation methods using growth factors are useful strategies for generating a DE with the ability to differentiate into hepatic or pancreatic lineages; however, these methods are not sufficient for generation of homogenous DE populations [46, 47]. To improve the efficiency of DE differentiation, several groups have attempted the modulation of expression levels in endoderm-related transcription factors. It has been demonstrated that overexpression of SOX17, which is an integral transcription factor for DE formation, promotes DE differentiation, resulting in an efficiency of DE differentiation of over 80 % based on the estimation of c-KIT/CXCR4 double-positive cells [47, 48]. The FOXA2 transcription factor also functions as a crucial regulator of the initial intracellular signaling pathways in DE differentiation [49, 50]. Overexpression of FOXA2 also enhances the efficiency of DE differentiation [51–53].

Several studies have demonstrated that, in the hepatic lineage specification stage, homogeneous hepatoblast populations can be generated by modulating the expression levels of hepatocyte-lineage-specific transcription factors as in the DE differentiation stage. Overexpression of HEX, which is an integral transcription factor for hepatic specification, has been shown to promote hepatic specification, resulting in enhanced expression levels of ALB and AFP in the HEX-transduced cells [54–56].

To generate functional hepatocyte-like cells which have characteristics similar to primary human hepatocytes, transduction of HNF4α genes, which are central regulators of liver development, in hESC-/hiPSC-derived hepatoblasts has been shown to successfully induce mature hepatocyte-like cells that have characteristics similar to

primary human hepatocytes [57]. Furthermore, the combination of overexpression of FOXA2 and HNF1α also could effectively induce mature hepatocyte-like cells [52]. The transduction of differentiation-related genes into hESCs/hiPSCs would be a powerful strategy to generate mature hepatocyte-like cells.

### 7.2.3 *Hepatic Differentiation from hESCs/hiPSCs by a Co-culture System*

In order to facilitate maturation of the hESC-/hiPSC-derived hepatocyte-like cells and to enhance the efficiency of hepatic differentiation, development of a differentiation system that more closely mimics progenitor development in vivo will be needed. The normal culture conditions of hepatocytes in vitro differ substantially from the environment in vivo. Cell–cell interactions are important in embryogenesis and organogenesis. In particular, heterotypic cell–cell interactions in the liver, such as interactions of parenchymal cells with non-parenchymal cells, play a fundamental role in liver function [58, 59]. Moreover, it is known that cell–cell interactions between the embryonic cardiac mesoderm and definitive endoderm are essential for liver development [60]. Transcription factors that are critical for hepatic development have been identified from these cell–cell interactions [60]. ES cells co-cultured with cardiac mesoderm showed spontaneous differentiation into hepatocyte-like cells [61]. It seems that the growth factors, including FGF and BMP, secreted from the cardiac mesoderm facilitate differentiation into hepatocyte-like cells. These results suggest that the combined differentiation methods, such as addition of soluble factors into the culture medium, transduction of differentiation-related genes, or co-cultivation with other lineage cells, may further enhance the differentiation and maturation efficiency of hepatocyte-like cells.

## 7.3 Hepatic Differentiation of hESCs/hiPSCs in Three-Dimensional Culture

Recently, numerous three-dimensional (3D) culture methods have been reported. Among these, the spheroid culture methods, which include the hanging-drop method and the float-culture method using culture dishes coated with non-adherent polymer, have been widely used to culture primary hepatocytes in vitro [62, 63] (Fig. 7.3). Spheroid culture methods allow better maintenance of the liver function of primary hepatocytes compared to two-dimensional (2D) culture [64, 65]. Moreover, various micro-patterned substrates, employing both surface engineering and synthetic polymer chemistry for utilizing spheroid culture, have been reported [66, 67] (Fig. 7.3). One of these technologies uses a nanopillar plate with an arrayed μm-scale hole structure at the bottom of each well and nanopillars that are aligned at the bottom of the respective holes. The seeded cells evenly drop into the holes,